

January 1978

Development of an erosion model and its application to phosphate mine dumps in southeastern Idaho

Vinod Prabhakar

Roland W. Jeppson

Loren R. Anderson

Follow this and additional works at: https://digitalcommons.usu.edu/water_rep



Part of the [Civil and Environmental Engineering Commons](#), and the [Water Resource Management Commons](#)

Recommended Citation

Prabhakar, Vinod; Jeppson, Roland W.; and Anderson, Loren R., "Development of an erosion model and its application to phosphate mine dumps in southeastern Idaho" (1978). *Reports*. Paper 150.

https://digitalcommons.usu.edu/water_rep/150

This Report is brought to you for free and open access by the Utah Water Research Laboratory at DigitalCommons@USU. It has been accepted for inclusion in Reports by an authorized administrator of DigitalCommons@USU. For more information, please contact digitalcommons@usu.edu.



DEVELOPMENT OF AN EROSION MODEL
AND ITS APPLICATION TO PHOSPHATE MINE
DUMPS IN SOUTHEASTERN IDAHO

by

Vinod Prabhakar 1/
Roland W. Jeppson
Loren R. Anderson

HYDRAULICS AND HYDROLOGY SERIES

UWRL/H-78/04

Utah Water Research Laboratory
College of Engineering
Utah State University
Logan, Utah

August 1978

DEVELOPMENT OF AN EROSION MODEL
AND ITS APPLICATION TO PHOSPHATE MINE
DUMPS IN SOUTHEASTERN IDAHO

by

Vinod Prabhakar ^{1/}
Roland W. Jeppson
Loren R. Anderson

The research reported herein was done under cooperative agreement 16 USC 581; 581a-581i between the USDA, Forest Service, Intermountain Forest and Range Experiment Station, Ogden, Utah and Utah State University. The financing was provided from SEAM funds by the Forest Sciences Laboratory, Logan, Utah to the Utah Water Research Laboratory at Utah State University to conduct the research

KEY WORDS: Erosion, Computer Simulation, Waste Disposal, Earthfill, Snowmelt, Mining Waste

ABSTRACT: Based on the equations of continuity and motion for sediment transport and the dynamic equation of spatially varied open channel flow, a computer simulation of erosion is developed. The water source for the erosion simulation may be rainfall or snowmelt. To provide snowmelt a computer simulation giving the rate of snowmelt from limited climatic data has been adapted to work conjunctively with the erosion model to provide a dynamic solution to erosion and overland flow, from precipitation and other limited climatic data. The computer simulation model has been tested using climatic data at and near the phosphate mine in Southeastern Idaho and calibrated from Forest Sciences Laboratory field erosion plot data at a spoil dump at the Wooley Valley Mine area. Good agreement exists between the erosion predicted by the model and the measured amounts over a season's time, but not on an individual storm, or day of heavy snowmelt basis.

^{1/} Research Assistant, Professor and Associate Professor of Civil and Environmental Engineering, Utah State University, Logan, Utah.

INTRODUCTION

Study Area

Strip Mining

During the past decade strip mining activities have increased very rapidly. Larger depths of overburden are being removed in order to reach the ore as large equipment makes this economically feasible and demands for the ore make it expedient. This trend of handling increasingly larger volumes of material will continue because:

1. Much of the more easily obtainable resources have been depleted.
2. Growth in worldwide population accompanied by industrialization have increased demands for fertilizers and other phosphate products.

The phosphate mines in Southeastern Idaho are one such industry where an increase in demand for phosphate has increased strip mining activity. Currently, the overburden material is being placed in spoil dumps. These dumps are large earthfill structures and are being placed in the rugged terrain of the mountains where phosphate is being mined.

Erosion of spoil dumps. Control of erosion from spoil dumps is of concern to the mining companies, the U. S. Forestry Service, and the general public. Erosion of spoil dump surfaces retards and in some cases prevents rehabilitation, thus creating scars on the landscape. In addition, the sediment eroded from the spoil dumps affects the downslope areas. In planning an effective erosion control scheme, it is necessary to know the physical properties of the dump surfaces and how these relate to erodibility of the soil under a given set of climatic conditions and the topography of the site.

Description of This Study

Purpose

The purpose of this study is to develop a mathematical model which describes erosion. The model developed herein has been implemented in the form of a computer program which simulates erosion on slopes of 3 horizontal to 1 vertical.

Erosion Data

Data obtained from a field study at the

Wooley Valley Mine, by the Forestry Sciences Laboratory on the U.S.U. campus, have been used in calibrating and verifying the computer model. The Forestry Sciences study measured the amount of soil eroded from plots under different surface treatments and from bare soil surfaces. Details of the treatment types and configuration of the erosion plots are provided in Appendix B. The erosion data taken by the Forestry Sciences study with no treatment (bare soil conditions) are used to calibrate the mathematical model developed in this study. After calibration of the mathematical model by use of the limited two years of data, it could be used to compute erosion from other key mine dumps.

Model Rationale

With respect to the design of the spoil dumps the questions that need to be answered are how the erosion rates are affected by gradient and slope length of the dump and the climate of the site. Accurate predictions of erosion rates are particularly difficult due to the large number of variables involved. Moreover, the mechanics of overland flow and erosion are not fully understood. Thus in mathematically modelling soil erosion some simplifying assumptions are necessary.

Assumptions. Since the soils at the mine sites display very little plasticity (Riker, Anderson and Jeppson, 1978) it is assumed that the soils are cohesionless. It is also assumed that the flow is one-dimensional and that the lateral inflow rate (from snowmelt or rainfall) and the infiltration rate are constants throughout the reach of overland flow under consideration.

Theory. The water surface profile is modelled by using the dynamic equation from spatially varied flow with lateral inflows, in open channels. This equation is solved numerically using the Hamming method. The numerical solution to the water surface profile equation is used in conjunction with the equations of continuity and motion for sediment transport to compute the erosion rates. Komura (1976) studied the erosion of cohesionless soils from a hydraulics point of view and derived theoretical equations for laminar and turbulent flow regimes. The approach employed by Komura was to relate the boundary shear stress caused by overland flow to the erosion rates via the use of the Kalinske bedload function (Rouse, 1949).

Date Requirements of Model

In using the model to make erosion computations the site topography climate and selected soil parameters are taken into consideration. The general data requirements for the model are summarized below.

Dump geometry. The pertinent dump geometric variables are:

1. Gradient
2. Slope length

Climatic data. Since most of the erosion problems occur in the springtime with snowmelt runoff, a snowmelt simulation is carried out. Hence, the climatic data includes the following:

1. Maximum daily temperature
2. Minimum daily temperature
3. Daily precipitation
4. Daily average humidity
5. Daily solar radiation

Soil parameters. The soil is assumed to be cohesionless:

1. Mean size diameter of slope soil
2. Specific gravity of slope soil

LITERATURE REVIEW

In its broadest sense erosion consists of entrainment and subsequent transport of a soil by natural agents such as wind and water. Erosion of soils has been studied from several perspectives and by people from several disciplines. As a result a voluminous amount of literature can be found pertaining to erosion of soils. Since this study is concerned with water as the erosive agent, all subsequent discussion will be limited to this aspect of soil erosion.

Erosion by Soil Detachment

The rate at which soil is removed by splash is considered to be a time-varying process by many investigators. The dependent factors are the raindrop intensity, size, duration and physical characteristics of the soil. Detachment of soil is caused predominantly by the momentum of the drops or the force per unit area exerted by the raindrops on the soil surface. Thus detachment is a function of the drop size and intensity of rainfall.

Some investigators have tried to relate the

detachment potential of soil to the kinetic energy of the raindrops. Wischmeier and Smith (1958) indicate that the kinetic energy of a rainstorm is a function of rainfall intensity. They suggest the following equation:

$$K_E = 916 + 331 \log i \quad \dots \dots \dots (2.1)$$

where

K_E = kinetic energy, in foot-tons per acre-in of rain

i = intensity of rainfall in inches per hour

Wischmeier and Smith further concluded that among the several different variables which affect soil loss the best single indicator of soil loss is the total raindrop energy of a storm and its maximum 30 minute intensity. This factor is called a rainfall erosion index (EI) and it reflects the combined potential force of the raindrop impact and the surface runoff to detach and transport soil particles from a field.

Osborn (1954) measured soil detachability by placing empty cans around soil samples under a rainfall simulator, thereby measuring the amount of soil splashed into the cans. He found that rates of soil detachability were lower on medium textured soils as compared to detachability of coarse or fine grained soils. In tests using an air-dry soil with a constant rainfall intensity of 4.8 in/hr, in which raindrop splash was referenced to time, Ellison (1944a) found that the maximum splash rate (i.e., soil removed by splashing water) occurred between 2 and 3 minutes after the rainfall began. Ellison's relationship of the weight of soil in raindrop splash as a function of rainfall duration, indicated that after the splash rate reached a maximum, it decreased rapidly. As the splash rate decreased, the weight of soil in the raindrop splash continued to vary slightly with time. Ellison concluded that the water reduced the cohesion between the surface particles causing them to go into suspension in the surface water. McIntyre (1958) on the other hand, found that the splash rates were not affected by the sealing of the surface. He attributed this partially to surface saturation which resulted in minimum cohesion. McIntyre used an air-dry soil and simulated rainfall intensities of 2.6 and 3.9 in/hr and found that both intensities produced a variation in the splash rate after a duration of about 20 minutes for the 2.6 in/hr rate and after 10 minutes for the 3.9 in/hr rate. McIntyre interpreted this to mean that the surface sealing had no effect on the initial splash rate. From his tests McIntyre concluded that the variation in splash rate indicates that four successive processes occur at the soil surface.

1. Rapid wetting of the surface causing low cohesion and high splash rates;
2. Formation of a crust on the soil surface

which decreases the splash rate and causing water to accumulate;

3. Removal of the crust (0.1 mm skin seal) by the turbulence in the water, hence, increasing the permeability of the surface;
4. Percolation of sufficient water to cause dissipation of drop energy on the soil once again and, hence, an increase in the splash rate.

Ellison (1944b) investigated the size of particles eroded by splash as compared to particle size eroded by runoff. Using plots 5 ft. long and 6 ft. wide, and varying simulated rainfall intensities and fall velocities of the raindrops, Ellison found that there was greater percentage of sand and gravel sized particles in the splashed sediment than in the original soil sample. When comparing the particle size in the runoff sediment to the particle size in the splash sediment, Ellison found a greater percentage of particles larger than 0.05 mm in the runoff sediment.

Rose (1961) studied the relationship between rainfall intensity and the aggregate structure of soils by using four types of soil and sieving them into four "structural fractions." Rose's goal was to compare, with the "structural fractions," the detachment of different soil types caused by the same simulated rainfall. By varying the rainfall intensity and duration, Rose found that both the soil type and size of the "structural fractions" can affect the amount of detachment and, hence, the rate of detachment. For a given rainfall intensity, Rose found that the detachment rate increased as the aggregate size decreased and by varying the intensity he noticed that the rate of detachment for the largest size was a linear function of rainfall intensity. For the other size, the detachment rate was non-linear and showed an increase in rate of detachment with an increase in rainfall intensity. From his results Rose concluded that the structural breakdown is more sensitive to rainfall intensity than to rainfall duration.

Soil detachment can also be caused by runoff. Ellison (1947) considered slope erosion to be dependent on the "detaching capacity" and "transporting capacity" of an erosive agent. In an investigation of a well compacted clay, he applied clear water to the upper end of the specimen. This applied water when introduced at the upper end of the slope represented maximum "transporting capacity" and minimum "detaching capacity" because the water was carrying no initial sediment and this resulted in very little erosion. In subsequent trials, when the water initially contained a maximum amount of soil, which would represent a maximum "detaching capacity" and a minimum "transporting capacity," again very little erosion was experienced. Ellison concluded that the maximum quantity of erosion will occur when the initial flow

contains just enough abrasive material to detach as much as the flow will have the capacity to add to its load.

Osborn (1955) is in general agreement with Ellison when he states that "the amount of soil transported depended on the transportability of the soil." Osborn concluded that the transporting capacity of the water depended on its volume, velocity and turbulence. He regarded the transportability of the soil as a function of the density, size and shape of the soil particles.

Affect of Slope on Erosion of Cohesionless Soils

The affect of slope on erosion of cohesionless soils has been the object of several studies, but the results of these studies are not always in complete agreement. The soil loss would be expected to be proportional to the slope, i.e., the steeper the slope the higher the soil loss.

Conner et al. (1930), after conducting erosion tests on uncompacted sandy soils indicated that the soil losses were directly proportional to the slope. Duley and Hays (1932) conducted a study using plots subjected to 1 in/hr of simulated rainfall at slopes varying from 0 to 2%. They, on the other hand, found that the amount of soil removed increased very slowly as the slope was increased to 4%. Increases in slopes above 4%, however, resulted in a rapid increase in the amount of soil eroded which indicated that a low velocity associated with slopes of low gradient, the water does not have the transporting capabilities it has at steeper slopes. As the slope increases, the velocity of water increases and even though the depth is less, there is more soil removed. However, Nichols and Sexton (1932), using artificial rainfall, ran tests on large plots (50 ft long by 15 ft wide) and found that the erosion varied uniformly with slope up to about 12%. Because the rate of erosion increased very rapidly above a slope of 12%, this slope was defined as the "critical slope" for the sandy silt soil.

Borst and Woodburn (1940), using both wet and dry uncompacted sandy loam and simulated rainfall, investigated the affect of slope on erosion by using test plots of 0.01 acres and varying the slope from 4.2% to 22.5%. By testing the soil in both wet and dry conditions, the initial moisture content of the soil was found to have no consistent affect on the amount of runoff or the amount of soil lost from the plots. Further, Borst and Woodburn found that the relationship between erosion and slope could be described as

$$E_s = 8.23 (S)^{1.223} \left\{ \begin{array}{l} \text{deg. sat.} = 100\% \\ \text{initially wet} \end{array} \right\} \quad (2.2a)$$

$$E_s = 4.84 (S)^{1.298} \left\{ \begin{array}{l} \text{deg. sat.} = 0\% \\ \text{initially dry} \end{array} \right\} \quad (2.2b)$$

where

E_s = quantity of erosion, in pounds by dry weight per acre

S = slope in percent

Because the rate of runoff was essentially constant for all the slopes it was concluded by Borst and Woodburn that the increase in erosion resulted from an increased velocity associated with increased slope.

Forrest and Lutz (1944) applied simulated rainfall to six plots with varying slopes and correlated the depth and velocity of flow water to the movement of soil particles. By maintaining the flowrate constant and increasing the slope, a decrease in the depth of flow was noted. Increase in slope was accompanied by an increase in erosion, with the exception of the 1.5% slope which lost less soil than either the 1% or 2% slopes. The test results of the study showed more large material (3.0 - 0.5 mm) transported on the 1% slope than on the 2.5% slope, whereas the loss of fine material was essentially the same for all slopes.

Meyer and Monk (1965) made laboratory studies of erosion by rainfall and shallow depths of flow as affected by slope, particle size and length of slope. Glass bead rather than soil was placed in a bed and the slope was varied from 0 to 20%. It was noted by Meyer and Monk that under certain values of slope and slope length the erosion was essentially zero. The erosion conditions were described by the modified power equations:

$$e_r = C_S (S - S_c)^m \quad \dots \dots \dots (2.3a)$$

and

$$e_r = C_L (L - L_c)^n \quad \dots \dots \dots (2.3b)$$

where

$$e_r = 0 \text{ when } L < L_c \text{ and } S < S_c$$

e_r = amount of soil eroded by runoff per unit width

C_S, C_L = constant coefficients

S = slope in percent

S_c = critical slope

n, m = constant exponents

L = length of slope

L_c = critical length of slope

Meyer and Monk concluded that runoff with rainfall caused more erosion for the smaller particles, but less erosion for the larger particles as compared to the same runoff without rainfall.

Forster and Martin (1969) conducted a study to determine the effect of unit weight of soil and slope on erosion. They used soils compacted to different degrees in simulated rainfall experiments. Based on the results and analysis of this study, the following conclusions, regarding the affect of unit weight of soil and slope on erosion of unprotected slopes, were reached:

1. The relationship between the weights of solids eroded and the slope indicates the existence of a unique slope from which a maximum amount of erosion will occur.
2. Analysis based on the average adjusted weight of solids eroded indicated:
 - a. On the flattest slope, the specimen compacted to be smallest unit weight experienced the highest rate of erosion.
 - b. On the steepest slope, the specimens compacted to the highest unit weight experienced the highest rate of erosion.

Komura (1976) conducted a study on the erosion of cohesionless soils from a hydraulics point of view and derived theoretical equations for both laminar and turbulent flow regimes. He further checked these equations against experimental data collected from erosion plots and found good agreement. Komura's work will be discussed in detail in Chapter 3 of this report.

Erosion of Cohesive Soils

The first attempts to investigate the scour or cohesive soils by water consisted of determining the highest flow velocity over a given clay bed before scour set in. The clays were defined roughly according to origin, consistency and possibly void ratio. Attempts were made to correlate the maximum permissible velocity against soil parameters, but field data soon showed that for the same clay the maximum permissible velocity could vary with geometry of the channel, depth of flow and other variables. The concept was abandoned as it was thought that the shear stress applied to the soil by flowing water might be a more fundamental erosive agent. Consequently, research concentrated on determining, for a given soil, the highest average boundary shear stress before scour set in.

This shear stress is called the "Critical Tractive stress, τ_c " and various soil classification and engineering parameters, such as plasticity index, percent by weight of clay, particle size, water content, void ratio, density and strength, etc., are related to it.

Lane (1955) summarized previous works in limiting velocities for non-cohesive and cohesive soils and presented it for stable channel design criteria. For channels in cohesive soils he tabulated values for this critical tractive stress as determined for the limiting velocities given by previous investigators. Of special interest was his attempt to correlate the critical stress to the void ratio of the soil.

Smerdon and Beasley (1959) applied the tractive stress theory to the stability of open channels in cohesive soils. Water was allowed to flow through a flume over a cohesive soil sample until bed failure was noted. Bed failure is described as "general movement of the bed material." The critical tractive stress was correlated to the plasticity index, mean particle size and percent clay.

Dunn (1959) utilized a submerged jet to determine the tractive resistance of cohesive sediments. The head of water on a nozzle placed vertically above the soil was increased until an initial erosion of the sample took place. The magnitude of the shear stress causing the scour was measured by replacing the sample by a shear plate coated with soil particles. The critical shear stress was then related to the vane shear strength of the soil, the mean grain size and the plastic limit. Dunn found that the physical properties of soil became more dependent on surface area and less dependent on weight as the size of the particles decreased.

Berghager and Ladd (1964) studied the erosion of cohesive soils through the use of flume tests. They postulated that the "shear failure" that occurred at the soil-water interface ought to be based on almost zero normal stress in order to help predict the behaviour of soil when exposed to running water. Boston Blue clay slurries were prepared in a fixed ring oedometer. The effective stress σ_v' in the soil was of the order of 3 to 5 kg/cm² depending on its weight. The soil sample was extruded with the porous stones from the oedometer and it was then placed on the platform whose inclination could be controlled, in a tank filled with water. The soil at any point is then acted upon by the bouyant weight of the soil above and by the upper porous stone. As the angle of inclination of the platform was increased (slowly to allow drainage), the applied shear stress will increase with a corresponding decrease in the effective normal stress in the soil, this type of

procedure was continued to failure. Berghager and Ladd made the following qualitative conclusions regarding the erosion of cohesive soil, i.e., the erosion of cohesive soils depends on:

1. Fabric of the soil
2. The grouping of the clay particles in flocs and aggregates
3. The nature of "true" cohesion
4. The influence of the stress history of the soil

Arulanandan et al. (1972) studied the influence of the chemical composition of the pore and eroding fluids on surface erosion. They developed an experimental procedure for measuring the erodibility of a soil, using a cylindrical soil sample which was placed in a cylinder. The region between the soil sample was filled with fluid of known chemical composition. The soil sample was then rotated so as to simulate sheet flow over a bare soil surface. The torque applied to the soil sample was related to the eroded soil material. The conclusions of this study were:

1. A critical shear stress exists for a given clay soil and eroding fluid below which surface erosion is essentially absent.
2. At applied shear stresses above the critical stress, over range studied, the erosion rate increases linearly.
3. Surface erosion is initiated as a particle by particle separation from the soil surface.
4. Both the sodium adsorption ratio (S.A.R.) and the concentration of pore fluid ions affect the critical stress for a given soil.
5. Concentrations of salts in the eroding fluid below that of the pore fluid reduce the critical shearing stress due to the swelling caused by the osmotic influences. The critical shear stress obtained by using distilled water as the eroding fluid is most conservative and most suited for situations where rain or snowmelt runoff is contemplated.

Soil Loss Equations

There are several "soil loss equations." These equations are usually formulated using data correlations through statistical techniques. The most popular one is the "universal soil loss equation" and it is stated as:

$$A = (RF)(K)(LS)^2(C)(PF) \dots \dots \dots (2.4)$$

where

A = average annual soil loss (tons/acres)
 RF = rainfall factor
 K = soil erodibility factor
 LS = length and steepness factor for the soil
 C = cropping and management factor
 PF = supporting conservation practice factor

Other equations of a similar nature have also been proposed by Wishmeier and Smith (1965), Musgrave (1947), Farnham, Beer and Heinemann (1966) and by Gottschalk and Brune (1950). In these equations the annual soil loss is correlated with rainfall, soil erodibility, length and steepness of slope, crop and crop management and soil management practices. A more detailed review of such equations is given by David (1972). According to Beer et al. (1966) such correlations usually are not comprehensive. The many possible variations in climate and watershed conditions are so great that it is impossible to develop a comprehensive correlation covering all types and gradations in variations. As a result errors of up to 400% are not uncommon with the use of such equations.

Trieste (1977) analyzed sediment data from 2805 infiltrometer plots to whether the Universal soil loss equation, a modified version of the Musgrave equation and a modified version of the Universal soil loss equation could be used to predict erosional losses. The results of this study indicate that "The soil loss equations are not universal, but for the most part, explain sediment yield with varying degrees of accuracy in different situations with no apparent trends or patterns."

Summary of Review of Literature

The review of literature presented in this report is by no means a comprehensive one, owing to the large amount of literature that is available on the subject of erosion of soil by water. Earlier research (1930-1950) was often conducted by soil scientists working with agricultural soils and the findings of investigators, especially those concerned with detachment of soil by raindrop impact, are especially difficult to apply to an erosion simulation scheme due to a lack of data regarding size and terminal velocity of raindrops. Also there is little information on the affect of slope length on the erosion characteristics. The affect of slope has been investigated by several researchers, however, the results of these studies are not in complete agreement. The soils at the phosphate mine sites in Southeastern Idaho display less plasticity than the range used to describe the erosion of cohesive soils, making it infeasible to use these results.

The approach used by Komura (1976) to mathematically model erosion seems to be the most

feasible, in that it can be extended to include the affect of site climate, topography and soil in computing erosion rates.

METHODOLOGY

Problem Statement

Objective

The purpose of this study is to develop a mathematical model which describes erosion. The erosive agent that undermines the surface stability of the overburden spoil dumps on the phosphate mines in Southeastern Idaho is runoff derived from spring snowmelt. Some erosion is also caused by runoff from rainstorm during the summer and fall season, but this is generally less than that caused by spring snowmelt.

Theoretical Framework

Model Rationale

Accurate predictions of erosion rates are particularly difficult due to the complexity of the phenomena. Thus in mathematically modelling erosion some simplifying assumptions are necessary.

Assumptions:

1. The overland flow is one-dimensional.
2. The slope of the dump face is constant.
3. The rainfall snowmelt and infiltration rates are constant throughout the reach of overland flow under consideration.
4. The pressure distribution in the water flowing over the surface is hydrostatic.
5. The composition of the soil is homogeneous.
6. The sediment is noncohesive.
7. The momentum correction factor in the direction of flow is constant and equal to 1.0.

Water surface profile equation. Under the above assumptions overland flow can be described by the open channel dynamic equation for spatially varied flow with lateral inflows.

$$\frac{dy}{dx} = \frac{S_o - S_f - 2qq^*/gy^2 + q^*UCos \phi/gy}{Cos \theta - q^2/gy^3} \quad . . (3.1)$$

where

S_o = the gradient or slope of the dump face
 S_f = the friction slope
 q = the combined flow rate per unit width
 q^* = the lateral inflow per unit area
 g = the gravitational acceleration
 y = the local depth of flow
 x = the distance along the dump face
 θ = the angle between the x-direction and the horizontal
 U = the velocity of lateral inflow as it enters the main flow
 ϕ = the angle between the x-direction and the velocity U

The variables of Eq. (3.1) are shown diagrammatically in Fig. 2.1.

The velocity of lateral inflow (U) as it enters the main flow is almost zero in the case where snowmelt provides the runoff. Also, it can be assumed that the rainfall is perpendicular to the overland flow, $\cos \phi \approx 0$, the fourth term in the numerator of Eq. (3.1) can be neglected.

Boundary shear stress distribution. The solution to Eq. (3.1) provides $y = f(x)$. From this the distribution of the boundary shear stress, as a function of distance along the slope, can be computed from the friction equation of open channel flow (Henderson, 1966).

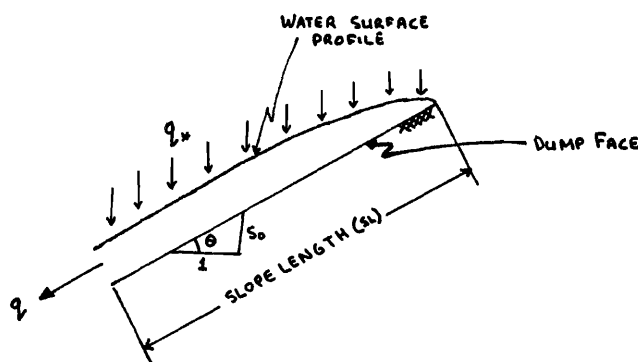


Fig. 3.1. A diagrammatic representation of the overland flow model.

$$\tau_o(x) = \gamma_w S_f y(x) \dots \dots \dots (3.2)$$

and,

$$\frac{d\tau_o}{dx} = \gamma_w \bar{S}_f \frac{dy}{dx} \dots \dots \dots (3.3)$$

where

$\tau_o(x)$ = boundary shear stress as a function of x
 y = the local depth of flow
 γ_w = the unit weight of water
 \bar{S}_f = the average friction slope

Continuity equation for sediment transport. This was expressed by Li and Simons (1973) to be a power function of the boundary shear stress.

$$\frac{dq_s}{dx} = a \tau_o^b \dots \dots \dots (3.4)$$

where

q_s = the rate of sediment transport in volume of material per unit time per unit width
 x = the distance in the downstream direction along the slope surface
 a = a constant describing the erodiability of the soil
 b = an exponent

Equation of motion for sediment transport. It can be expressed in the form of the Kalinske bedload function (Rouse, 1949).

$$\frac{q_s}{U_* D} = a_s \left[\frac{U_*^2}{(\frac{\sigma}{\rho} - 1) y D} \right]^P \dots \dots \dots (3.5)$$

where

U_* = the friction velocity
 D = the mean sediment size
 σ and ρ = the densities of sediment and water, respectively
 P = a dimensionless exponent
 a_s = a constant
 y = depth of flow

According to Kalinske and Brown (1949), $a_s = 10$

and $P = 2$ for erodible open channels.

Since $U_* = \sqrt{\tau_o / \rho}$, Eq. (2.5) can be rewritten as:

$$q_s = \frac{a_s}{\left[\left(\frac{\sigma}{\rho} - 1 \right) g \right]^P D^{(P-1)}} \left[\frac{\tau_o}{P} \right]^{(2P+1)/2} \quad (3.6)$$

Combining the equations of continuity and motion. The differential equation of sediment transport is obtained by differentiating Eq. (3.6) with respect to x and equating the result to Eq. (3.4), giving:

$$\frac{dq_s}{dx} = a \tau_o^b = \left[\frac{(1+2P) a_s}{2\rho^{(1+2P)/2} \left[\left(\frac{\sigma}{\rho} - 1 \right) g \right]^P D^{(P-1)}} \frac{d\tau_o}{dx} \right]$$

$$\tau_o^{(2P-1)/2} \dots \dots \dots (3.7)$$

From whence:

$$a = \frac{(1+2P) a_s}{2\rho^{(1+2P)/2} \left[\left(\frac{\sigma}{\rho} - 1 \right) g \right]^P D^{(P-1)}} \frac{d\tau_o}{dx} \quad (3.8)$$

and

$$b = \frac{2P-1}{2} \dots \dots \dots (3.9)$$

Rate of soil erosion. The volumetric erosion rate per unit area can be expressed as:

$$E_v = \frac{C_f}{SL} \int_o^{SL} a \tau_o^b dx \dots \dots \dots (3.10)$$

where

C_f = a field calibration coefficient

E_v = volumetric erosion rate per unit area of the slope. Since a unit width is being used dx represents the area dA with the dimensions of weight

The erosion rate per unit area per unit time is computed by multiplying the volumetric erosion rate by the dry unit weight of the soil.

$$E_R = \gamma_d C_f E_v \dots \dots \dots (3.11)$$

where

E_R = the erosion rate per unit area of the slope face (weight per unit area per unit time)

γ_d = dry unit weight of the soil

Numerical Solution of W.S.P.¹ Equ.

Boundary Condition

Assuming that uniform flow conditions ($S_f = S_o$) exist at the downstream end of the slope, the normal depth can be computed from Chezy's equation and used to start the numerical solution.

$$V = C_c \sqrt{S_o y_o} \dots \dots \dots (3.12)$$

where

V = the average velocity

y_o = the normal depth

S_o = the slope

C_c = Chezy's 'C-value' ($= \sqrt{8g/f}$)

f = Darcy Weisbach friction factor

Since $q = Vy_o$, Eq. (2.12) may be rewritten as:

$$y_o = (q^2 f / 8g S_o)^{1/3} \dots \dots \dots (3.13)$$

Friction factor. It is well known that for laminar flow, the Darcy Weisbach friction factor is a linear function of the Reynolds number.

$$f = \frac{C}{Re} \dots \dots \dots (3.14)$$

where

C = a constant for a given slope and soil surface roughness

Re = Reynolds number

For laminar flow over smooth surfaces with small bed slopes, the theoretical value of $C = 24$ has been verified by several investigators (Hopf, 1910; Jeffreys, 1925; Horton et al., 1935; Allen, 1934; Straub et al., 1958). Other studies in rough steep channels with cross-sectional shapes other than rectangular show discrepancies from the theoretical value of C . Chow (1959) noted the trend of variation of the C value, i.e., higher for rougher channels and also, higher for rectangular than for triangular channels.

Chen (1975) studied the affect of slope on the C value for two species of turf, in addition to data from other investigators' studies and found the following functional form:

$$C = \alpha S_o^\beta \dots \dots \dots (3.15)$$

in which α and β are parameters which depend on the roughness size and the rainfall intensity, if

¹ W.S.P. = Water Surface Profile

under rain. Chen suggests the following equation from the data of Woo and Brater's (1961) glued sand surface study:

$$C = 235 S_o^{0.296} \text{ for } S_o \geq 0.00045 \quad \dots (3.16a)$$

$$C = 24 \text{ for } S_o < 0.00045$$

and for the 2 species of turf:

$$C = 510,000 S_o^{0.662} \text{ for } S_o \geq 0.00000029 \quad \dots (3.16b)$$

$$C = 24 \text{ for } S_o < 0.00000029$$

Chen further indicates that the α value in Eq. (3.16) approaches 24 under no rainfall conditions, and the β value approaches zero for perfectly smooth surfaces. The under uniform flow conditions available on the C value are summarized in Table 3.1.

Bare soil surfaces exhibit a greater roughness than glued sand surfaces, and a lower roughness than turf. Hence, the C value for bare soil surfaces may lie between 235 and 510,000. A laboratory study was undertaken to determine the C value for bare soil surfaces.

Table 3.1. A range of C values (after Chen, 1975)

Surface Type	C Value
Glued Sand	235
Turf	510,000

Laboratory Study

The facilities used to conduct this laboratory study were provided by the Utah Water Research Laboratory in Logan, Utah. A detailed description of these facilities is given below.

The objective. The object is to determine the affect of flow rate, normal depth and slope on the C value. This relationship can be presented by combining Eqs. (3.13) and (3.14).

$$C = \frac{8gy_o^3 S_o Re}{2q} \quad \dots (3.17)$$

Since $Re = q/\nu$ (ν = kinematic viscosity of water), Eq. (3.17) may be rewritten as:

$$C = \frac{8gS_o y_o^3}{q\nu} \quad \dots (3.18)$$

The method employed is to set the slope (S_o), vary the flowrate (q) and measure the normal

depth (y_o).

Apparatus. The laboratory facility used for the tests consists of 20 ft. (6.096 m) square tilting bed hinged at the downstream side and supported on hydraulic cylinders near the upstream tank. The test bed can support a 1 foot deep soil layer. Water can be applied as a constant flow through a head tank at the upstream end of the test bed. The runoff from the test bed exists through ten 2-ft (60.96 cm) wide channels at the downstream end of the test bed. The side walls of the test bed are built of plexiglass to permit visual examination of the surface flow.

Water enters the test bed through a baffled head tank which has dissipated sufficient energy in the water to permit a quiet, smooth approach over the soil surface. The head tank is coupled with a supply line with flexible tubing to permit the test bed to be tilted to desired slopes.

A data collection system consists of a discharge-measuring magnetic flux meter and 20 depth-measuring manometers.

Along the centerlines of the third and eighth 2-ft (60.96 cm) exit sections, two rows of ten depth-measuring manometer tubes were installed on the test, spacing 2 ft (60.96 cm) apart. Each of the 1/2 in. aluminum manometer tubes on bed side extend through the soil layer. The top of the tube is capped with fine mesh brass screen, level with the soil surface; across the bottom of the test bed is a flexible plastic tube which connects the bottom of the manometer tube. The 1/2 in. manometer tube (plastic) is pivoted to the side wall of the test bed to maintain in the vertical position when the bed is tilted. Before starting any experiment, the manometer tubes are first filled with water to the soil level in the bed.

Range of variables.

1. Flowrate (Q) - 0.33 cfs to 1.27 cfs (or 0.0165 cfs/ft to 0.0635 cfs/ft).
2. Slope (S_o) - 0.3333 (or 3:1).

A typical experimental run. The slope of the tilting bed flume is set at 0.3333. The head tank is filled to within a few inches to the top. The two rows of the first five manometers, from the downstream end are filled with water to the soil surface, and the initial reading is recorded. The valve is then set to desired position, to give the flowrate which is monitored by means of a magnetic flux meter in the line. As the water begins to flow over the soil surface and stabilizes (about 5 minutes) a final reading is taken from the manometers.

Observations. Sheet flow conditions exist only for a very short time, after which it is channelized into rills and excluded some of the

manometers from the flow. The flow varied from laminar to turbulent, depending upon the position on the tilting bed. This is due to localized changes of the relative roughness (K_s/y) as sediment is eroded.

Results. The depth vs. discharge relations are presented in Figs. 3.2-3.5 and Table 3.2. The use of Eq. (3.18) yields no valuable information about the C-value for bare soil surfaces. This is primarily due to the changes in the bed configuration as the soil is eroded by flowing water. First, as channelization occurs the actual flowrate (q) value departs from the computed value of the flowrate. Also, as the soil is eroded the measured value of the depth (from the original soil surface) is also different from the actual value of the depth.

Discussion of results. The C value is a function of the surface roughness (K_s) and the slope (S). As the soil is eroded the surface roughness changes. Hence, the surface roughness for bare soils is dependent upon the scouring capability of the water. The scouring capability of water is, in turn, related to the flowrate and depth of flow. Also, occurrence of both laminar and turbulent flow regimes is highly dependent upon the pattern of channelization. The channelization is a two-dimensional affect and, since its influence is substantial, the assumption that the overland flow is one-dimensional could give rise to errors in the model.

In viewing the flow patterns (laminar and turbulent) on the tilting bed, it is felt that classifying the flow as being in the transition zone might facilitate a rationale manner for computing the normal depth. The Colebrook-White equation, which describes some basic fluid friction relationships in the transition zone is considered.

Colebrook-White equation. The form of this equation is:

$$\frac{1}{\sqrt{f}} = 1.74 - 2 \log_{10} \left[\frac{K_s}{4y_o} + \frac{18.7}{\text{Re} \sqrt{f}} \right] \quad \dots (3.19)$$

where

$K_s/4y_o$ = the relative roughness for open channel flow

y_o = the depth of overland flow

K_s = the soil surface roughness

The friction factor can be solved for using Chezy's equation and the relationship $C_c^2 = 8g/f$

$$f = \frac{8gS_o y_o^3}{q^2} \quad \dots (3.20)$$

Substituting Eq. (3.20) into Eq. (3.19) and solving for $K_s/4y_o$:

$$\frac{K_s}{4y_o} = 10^{(0.87 - 0.5/\sqrt{8gS_o y_o^3/q^2}) - 18.7/\text{Re} \sqrt{8gS_o y_o^3/q^2}} \quad \dots (3.21)$$

The data collected, namely q vs. y , in the laboratory study is used to compute K_s/y_o in Eq. (3.21). The main motive for computing $K_s/y_o = f(y_o, q)$ is to replace K_s in Eq. (3.19) with this functional relation, since K_s is very hard to measure. The results of this computation are shown in Fig. 3.6 and Table 3.3.

$$B = 0.1641 [q]^{0.6831}, r^2 = 0.9743 \quad \dots (3.22)$$

Hence, the relationship of y and K_s can be expressed as:

$$y_o = B + 0.13 K_s \quad \dots (3.23)$$

or

$$K_s = \frac{y_o - B}{0.13} = \frac{y_o - 0.164 q^{0.683}}{0.13} \quad \dots (3.24)$$

Computation of normal depth. Substituting Eq. (3.24) and Eq. (3.25) into Eq. (3.19) yields an implicit equation for the normal depth (Y_o).

$$\frac{1}{\sqrt{8gS_o y_o^3/q^2}} = 1.74 - 2 \log_{10} \left[\frac{y_o - B}{0.13 y_o} + \frac{18.7}{\text{Re} \sqrt{8gS_o y_o^3/q^2}} \right] \quad \dots (3.26)$$

Table 3.3. y vs. K_s , as computed from laboratory data and the Colebrook-White equation, and fitted using regression techniques

Set #	Normal depth $y_o = f(K_s)$ [ft.]	Flowrate q (cfs/ft)	Correlation coefficient
1	$y_o = 0.009203 + 0.13 K_s$	0.0165	0.999
2	$y_o = 0.020327 + 0.1289 K_s$	0.046	0.999
3	$y_o = 0.024287 + 0.13 K_s$	0.0635	0.999
4	$y_o = 0.012821 + 0.126 K_s$	0.0208	0.999

Table 3.2. A summary of data collected; depth vs. discharge relations.

Run Number	Flowrate (ft ³ /sec-ft)	Manometer number	South side of tilting flume	North side of tilting flume
			Depth (in.)*	Depth (in.)*
1	0.0165	1	0.1	0.29
1	0.0165	2	-	1.14
1	0.0165	3	-	0.95
1	0.0165	4	-	0.57
1	0.0165	5	0.86	-
1	0.046	1	0.1	0.67
1	0.046	2	1.14	1.90
1	0.046	3	-	-
1	0.046	4	1.81	0.76
1	0.046	5	1.81	0.29
1	0.0635	1	0.86	1.05
1	0.0635	2	-	1.81
1	0.0635	3	0.29	-
1	0.0635	4	1.66	0.76
1	0.0635	5	1.90	0.29
2	0.0208	1	0.85	0.85
2	0.0208	2	0.28	0.76
2	0.0208	3	-	-
2	0.0208	4	0.57	0.66
2	0.0208	5	-	0.47
2	0.0234	1	-	-
2	0.0234	2	-	0.57
2	0.0234	3	-	-
2	0.0234	4	0.60	0.28
2	0.0234	5	1.8	-
2	0.0395	1	0.95	0.28
2	0.0395	2	-	-
2	0.0395	3	0.95	-
2	0.0395	4	0.76	0.19
2	0.0395	5	2.18	-

*; Dashes (-) indicate missing data due to channelization.

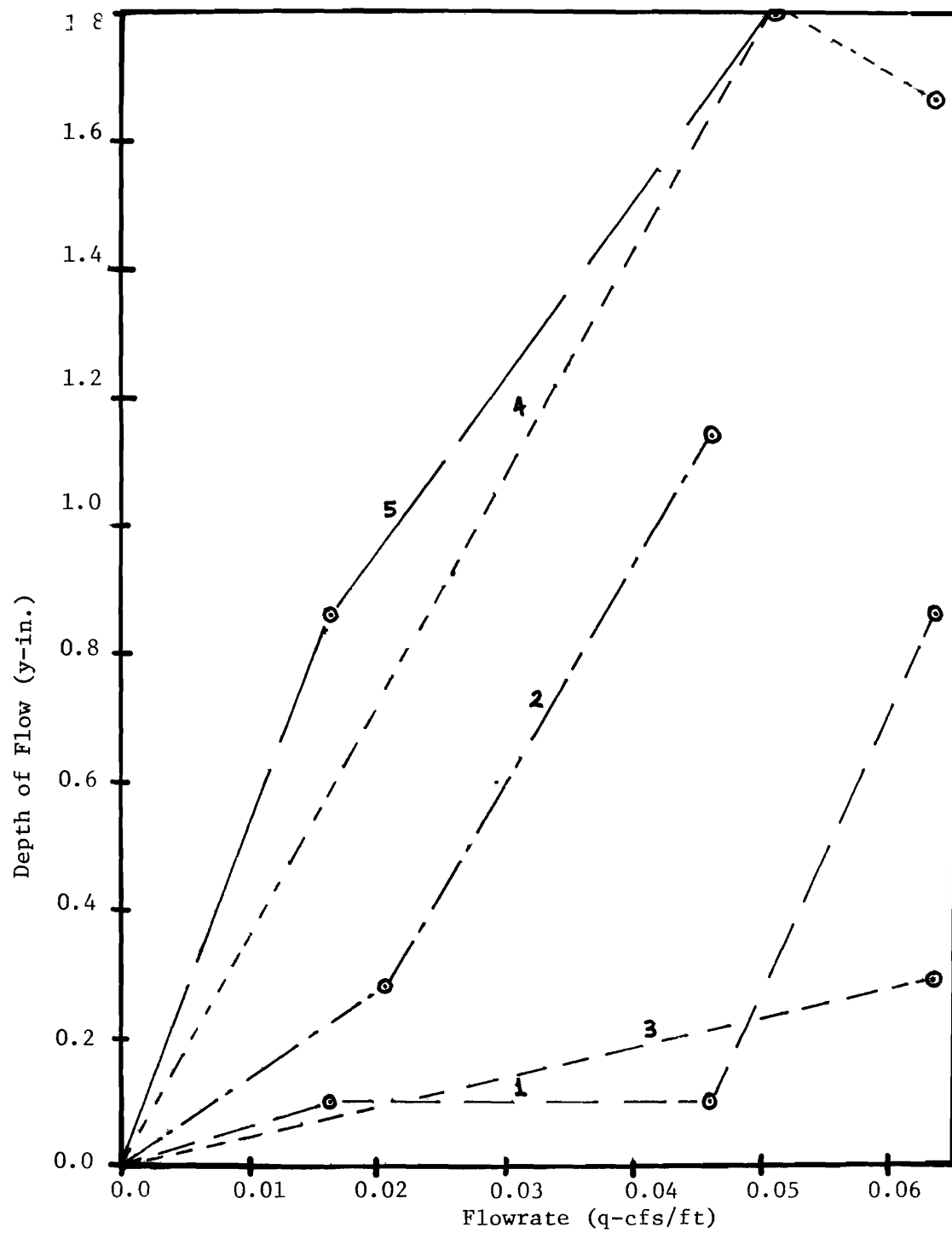


Fig. 3.2. Depth vs. discharge, test #1, southside of flume

(numbers along the lines indicate manometer #)

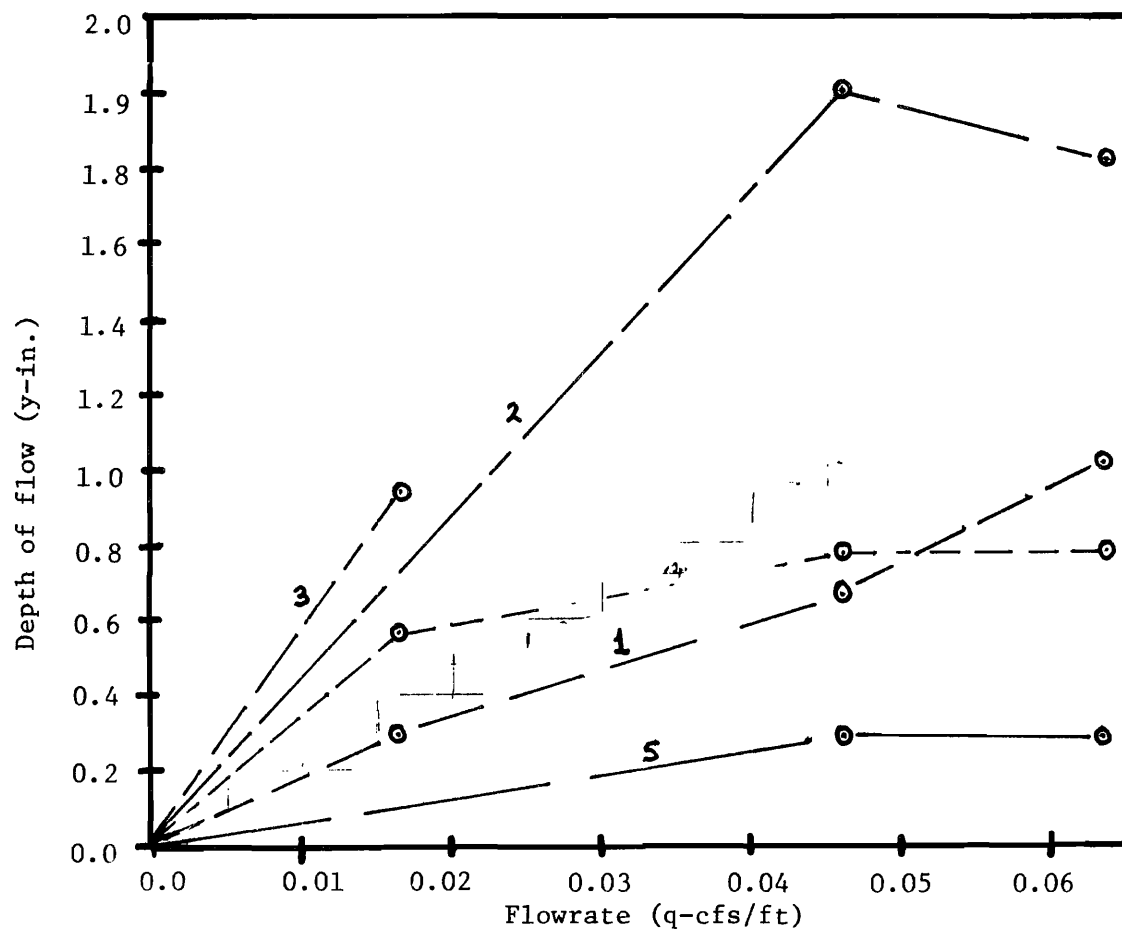


Fig. 3.3. Depth vs. discharge, test #1, north side of flume.

(numbers along the lines indicate manometer #)

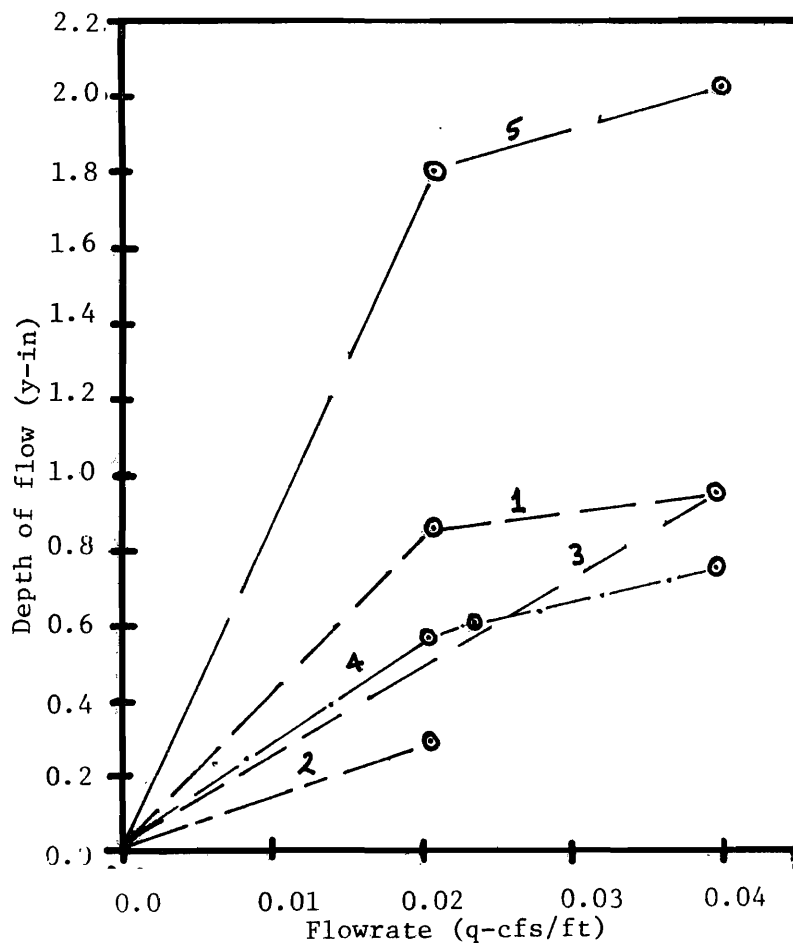


Fig. 3.4. Depth vs.. discharge, test #2,
south side of flume
(numbers along the lines indicate manometer #)

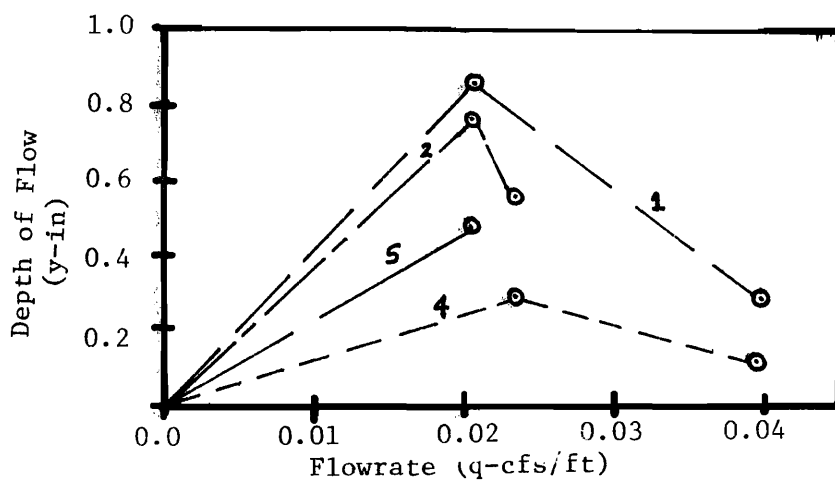


Fig. 3.5. Depth vs. discharge, test #2,
north side of flume

(numbers along the lines indicate manometer #)

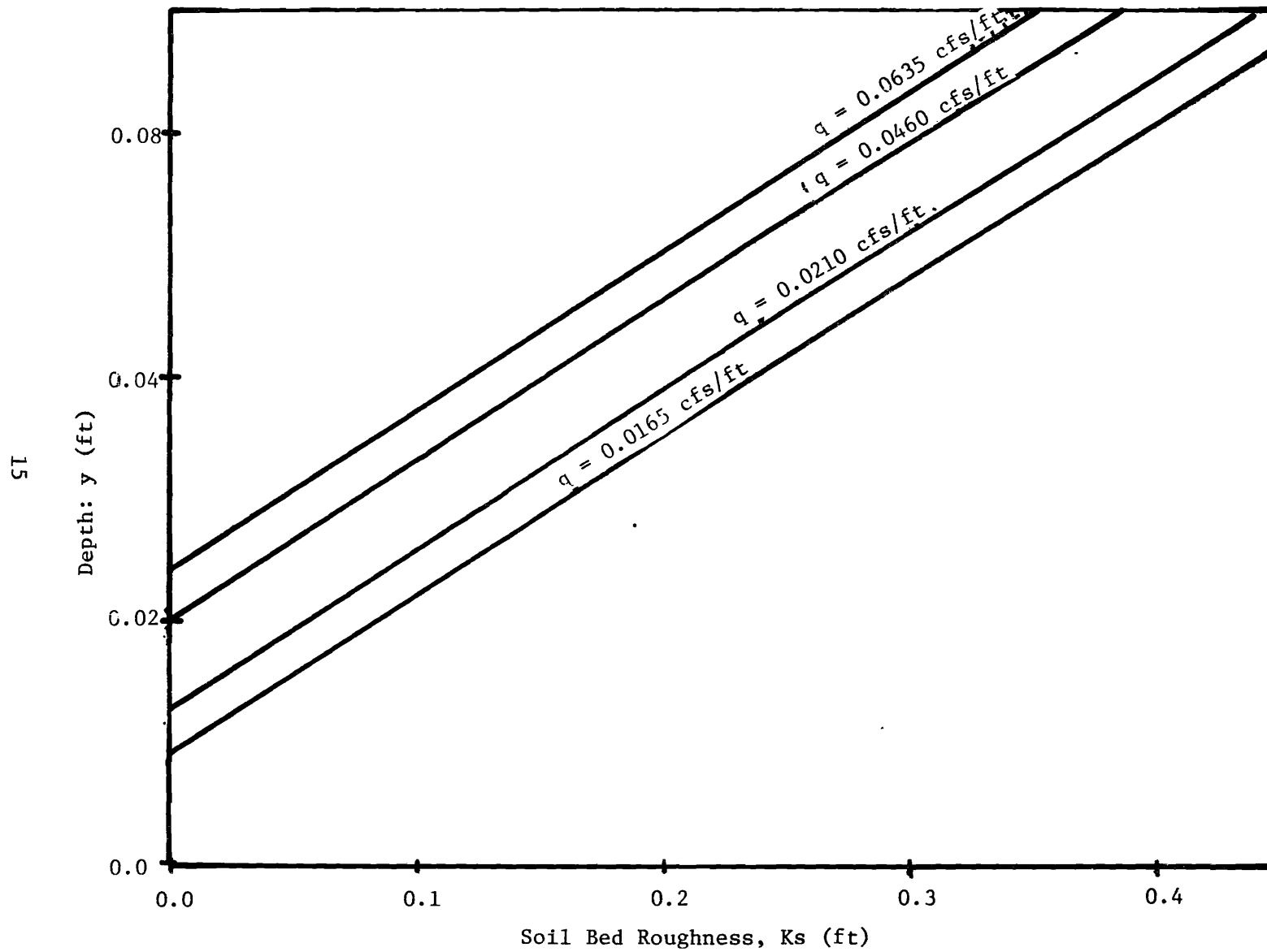


Fig. 3.6. y vs. K_s , as computed from the Colebrook-White equation and laboratory data

The normal depth is solved from Eq. (3.22) using the Newton Raphson method,

$$y_o^{(m+1)} = y_o^{(m)} - \frac{F}{\partial F / \partial y_o} \quad \dots \quad (3.27)$$

where

$$F = \frac{1}{\sqrt{8gS_o y_o^{3/q}}} - 1.74 + 2 \log_{10} \left[\frac{y_o - B}{0.13 y_o} + \frac{18.7}{\text{Re} \sqrt{8gS_o y_o^{3/q}}} \right] \quad \dots \quad (3.28)$$

and,

$$\frac{\partial F}{\partial y_o} = - \frac{1.5}{\sqrt{\frac{8S_o}{q^2} y_o^{2.5}}} + \frac{2 \log_{10}(e)}{\left[\frac{y_o - B}{0.13 y_o} + \frac{18.7}{\text{Re} \sqrt{\frac{8S_o}{q^2} y_o^{2.5}}} \right]} \quad \dots \quad (3.29)$$

m = iteration number

3 = 2.718 (base to natural logarithm)

Solution Process

The first order differential equation, to which a solution is sought, is available in the following form:

$$\frac{dy}{dx} = \frac{S_o - S_f - 2qq*/gy^2}{\cos \theta - q^2/gy^3} \quad \dots \quad (3.30)$$

The Hamming method is used to generate the numerical solution to the above equation.

The Hamming method. The first value of y is the normal depth and it is available. The next three values of y and dy/dx in the upstream direction are generated using the Euler method. These four values are then used to compute the predicted solution using the fourth order Milne predictor.

$$1. \text{ Predictor } - y_{i+1}^{(o)} = y_{i-3} + \frac{4}{3} \Delta x \left. \frac{dy}{dx} \right|_i - \left. \frac{dy}{dx} \right|_{i-1} + 2 \left. \frac{dy}{dx} \right|_{i-2} \quad \dots \quad (3.31)$$

The predicted value is modified, by assuming that the local truncation error on successive intervals does not change appreciably.

$$2. \text{ Modifier } - y_{i+1}^{(o)} = y_{i+1}^{(o)} - \frac{112}{121} (y_o^{(o)} - y_i^{(2)}) \quad \dots \quad (3.32)$$

The modified value of y is then acted upon by the Hamming corrector.

$$3. \text{ Corrector } - y_{i+1}^{(J)} = \frac{1}{8} 9y_i - y_{i-2} + 3\Delta x \left[\left. \frac{dy}{dx} \right|_{i+1}^{J+1} + 2 \left. \frac{dy}{dx} \right|_i - \left. \frac{dy}{dx} \right|_{i-1} \right] \quad \dots \quad (3.33)$$

The final value of y is then obtained by estimating the truncation error from the y values given by the predictor and the corrector.

$$4. \text{ Final } - y_{i+1} = y_{i+1}^{(n)} + \frac{9}{121} [y_{i+1}^{(o)} - y_{i+1}^{(J)}] \quad \dots \quad (3.34)$$

The above method has been implemented in the form of a computer program (Appendix A).

Step size. Experience with the solution process indicates that a step size (Δx) of -0.03125 ft or smaller ensures that the error criteria (0.001) is satisfied. The program is built in such a way that if the error criteria is not satisfied the step size is decreased by a half. This division of the step size is carried out until the error criteria is met. On the other hand, if the error criteria is large compared to the truncation error, then the step size is enlarged.

Computation of friction slope. The friction factor (f) is computed from the Colebrook-white equation (Eq. 3.19). This is an implicit equation in f. The Newton Raphson method is employed to solve for f, with y and q as knowns.

$$f^{(m+1)} = f^{(m)} - \frac{F(f)}{\partial F(f)} \quad \dots \quad (3.35)$$

where

$$F(f) = \frac{1}{\sqrt{f}} - 1.74 + 2 \log_{10} \left[\frac{y-B}{0.13y} + \frac{18.7}{\text{Re}\sqrt{f}} \right] \quad \dots (3.36)$$

$$\frac{\partial F(f)}{\partial f} = -\left(\frac{1}{2}\right) \frac{1}{f^{3/2}} + \frac{2 \log_{10}(e)}{\left[\frac{y-B}{0.13y} - \frac{18.7}{\text{Re}\sqrt{f}} \right]} - \left[\frac{18.7}{2 \text{Re} f^{3/2}} \right] \quad \dots (3.37)$$

When the change in f from iteration to iteration is smaller than 0.0001, the f value is then used to compute the friction slope from Chezy's equation

$$S_f = q^2 f / 8gy^3 \quad \dots (3.38)$$

Model Construction

The model developed in this study is implemented in the form of a computer program. The essentials of the computer model can be expressed in the form of a flow diagram (Fig. 3.7).

The computer model operates on a daily basis over a period of one year, from August 1 to July 30. A listing of the computer program is provided in Appendix A.

Dump Geometry

The pertinent dump geometric variables read in include:

1. The gradient
2. The slope length
3. The slope aspect (North, South or West facing slopes)

Flowrate Computation

Basically two different schemes are employed to compute the flowrate depending upon the time of the year. The flowrate that causes erosion comes from spring snowmelt and rainstorms in the summer and fall seasons. The snowmelt flowrate computation is preceded by snowmelt simulation.

Snowmelt simulation. Jeppson, Hill and Israelsen (1974) developed a snowmelt simulation model as a part of their study. This computerized snowmelt model estimates the snowmelt processes as affected by:

1. Slope aspect
2. Daily air temperature
3. Windspeed
4. Humidity
5. Precipitation
6. Solar radiation

Data availability. No comprehensive climate stations exist in the vicinity of the phosphate mines in Southeastern Idaho. In fact, only precipitation and air temperature data are available at the Wooley Valley Mine that has been collected by Triangle Mining Company in an unofficial capacity. The lack of windspeed, humidity and solar radiation data makes it difficult to accurately assess existing hydrologic conditions which influence snowmelt processes. Hence, the windspeed and humidity data are taken from Pocatello, Idaho, and solar radiation from Logan, Utah.

Sensitivity analysis. Several simulations are made, with various coefficients to humidity and windspeed data, to study the sensitivity of the snowmelt model to these parameters. The results of this analysis (Fig. 3.8-3.10) indicate that the annual snowmelt is not greatly influenced by windspeed and humidity. Hence, this snowmelt simulation model is incorporated into the erosion model developed in this study.

Snowmelt flowrate. In actuality snowmelt will occur mostly during a short period in the day. Due to a lack of actual data, there is no rational basis for arriving at the time base over which the snowmelt might occur. It is felt that this time base may vary with the time of the year during the snowmelt period. Hence, a triangular hydrograph with a time base of 2 hours is used. Since 1 acre-in. is approximately 1 cfs-hour, the peak flowrate is computed thus:

$$q_{*s} = f_r d_s \quad \dots (3.39)$$

where

- q_{*s} = snowmelt lateral inflow rate per acre of melt area (ft³/sec-acre)
- d_s = total daily snowmelt runoff (inches)
- f_r = runoff coefficient (dimensionless)

Low infiltration rate of the soils at the site indicates that very little runoff will percolate into the fill. Hence, the runoff coefficient of 0.9 is used.

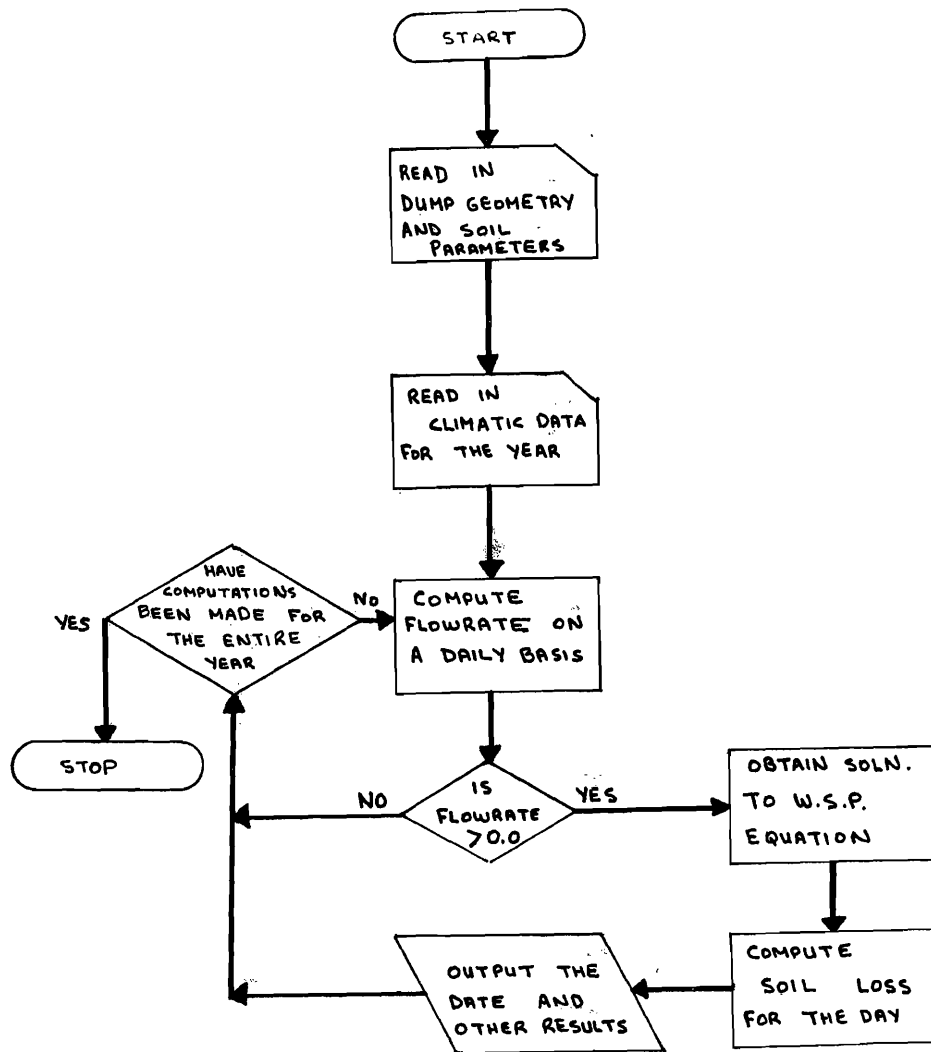


Fig. 3.7. A simplified flow diagram of the erosion model.

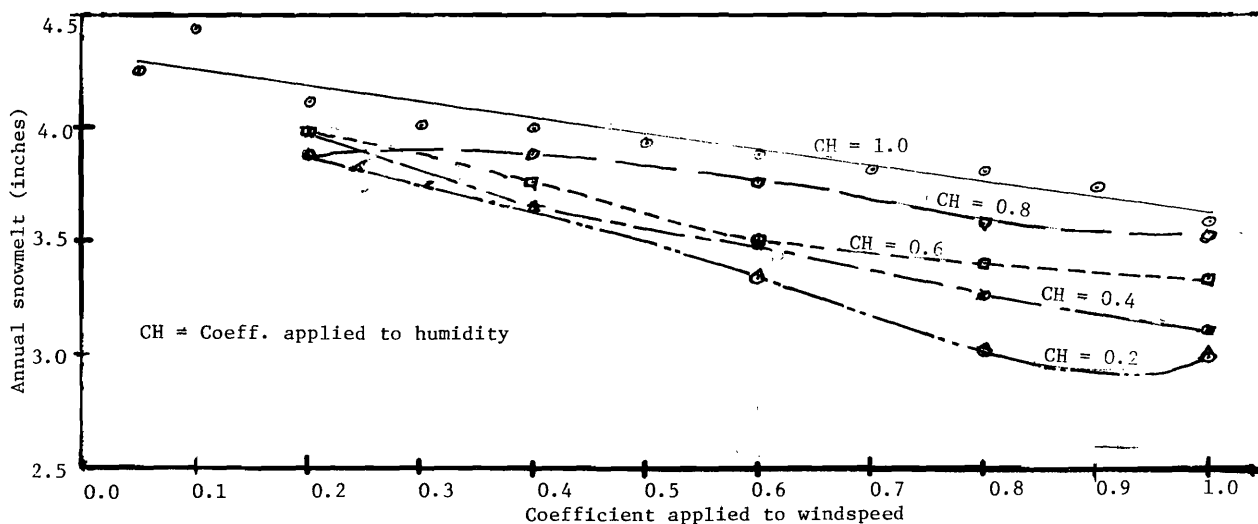


Fig. 3.8. Snowmelt as function of windspeed and humidity on a horizontal face.

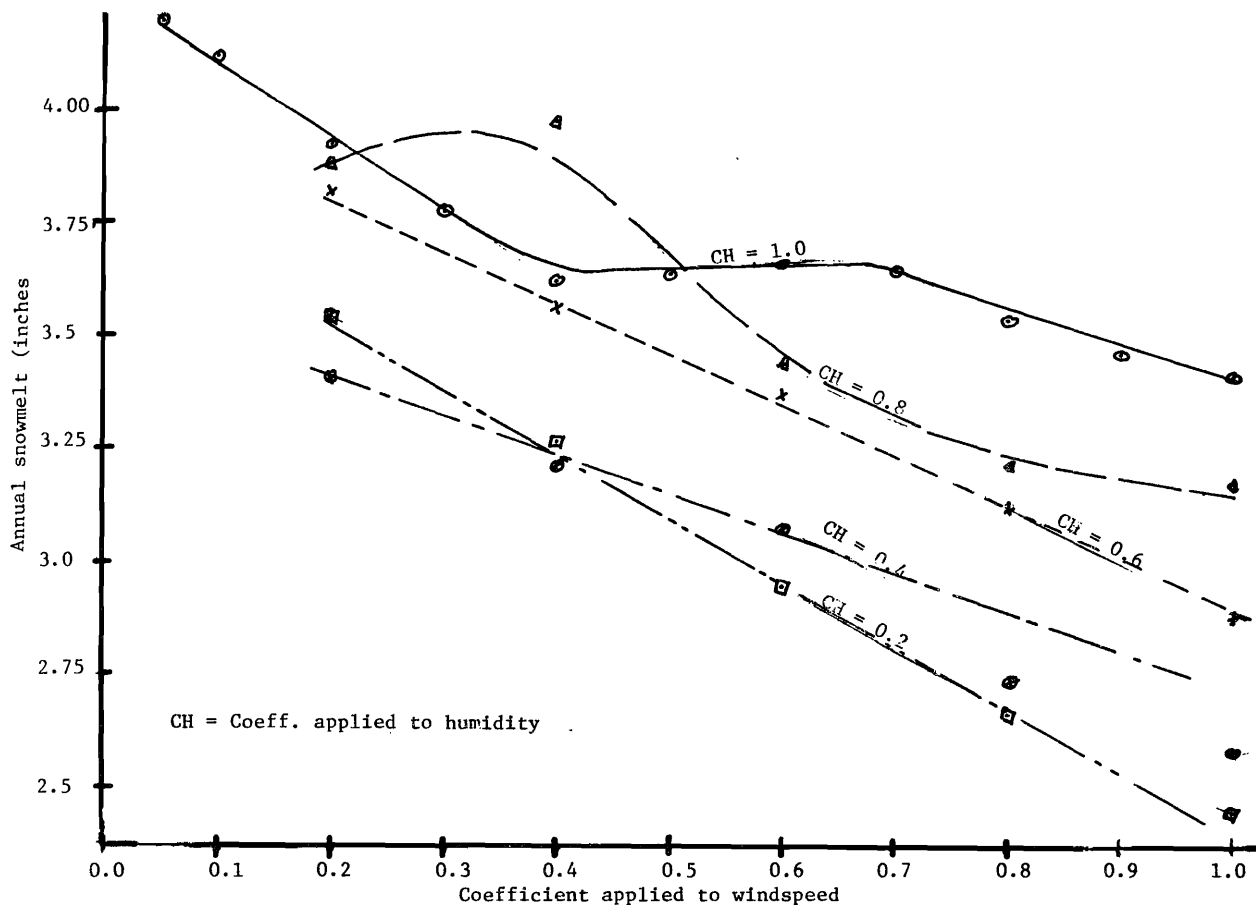


Fig. 3.9. Snowmelt as function of windspeed and humidity on a northface

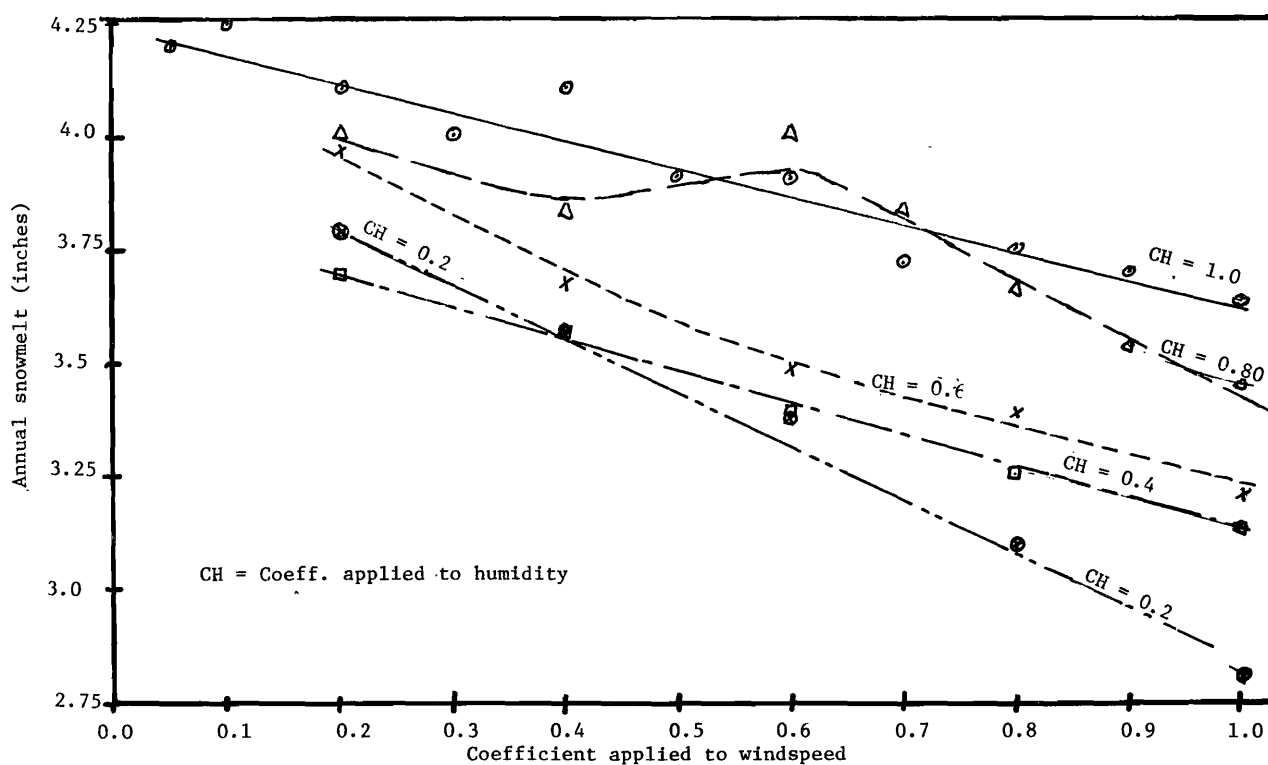


Fig. 3.10. Snowmelt as a function of windspeed and humidity on a west face

The one-dimensional flowrate over the slope is then obtained from the total flowrate:

$$q = \frac{q_{*s}(SL)}{43560} \quad (3.40)$$

where

q = one-dimensional flowrate or flowrate per unit width of slope

SL = slope length

$43560 = \text{ft}^2$ in an acre

Rainfall flowrate. This is considerably more difficult to compute, due to the erratic nature of the rainstorms with respect to intensity, duration and time history, in the mountainous terrain where the phosphate mines are located. The only information available on the summer and fall rainstorms is the total depth, duration and the maximum 5 minute intensity. Hence, the rainfall flowrate computation is based on a triangular hydrograph with 2 hours as the time base. Since 1 acre-in. is approximately 1 cfs hour.

$$q_{*r} = \frac{d_r}{r_d} f_r \quad (3.41)$$

where

q_{*r} = rainfall lateral inflow rate per acre of dump face

d_r = total depth of storm

t_d = total time duration of storm (hours)

The one-dimensional flowrate over the slope face is computed thus:

$$q = \frac{q_{*r}(SL)}{43560} \quad (3.42)$$

Computation of Erosion Rate

Numerical Integration

The integration indicated in Eq. (3.10) is performed numerically. A fourth order Newton forward scheme is used to start the integration. In the middle a fourth order Stirling central formula is employed. At the end a fourth order Newton backward technique is used (Fig. 2.8).

Newton forward. Uses information to right of $x = 0$ to perform the integration.

$$E_2 = \Delta x [0.375 F_1 + 19 F_2/24 - 5F_3/24 + F_4/24] \quad (3.43)$$

Stirling central. Uses information on both sides of a point to perform the integration.

$$E_i = E_{i-1} + \Delta x [13(F_{i-1} + F_i)/24 - (F_{i-2} + F_{i+1})/24] \quad (3.44)$$

Newton backward. Uses information to the left of $x = SL$ to perform the integration.

$$E_n = E_{n-1} + \Delta x [3F_n/q + 19 F_{n-1}/20 - 5F_{n-2}/24 + F_{n-3}/24] \quad (3.45)$$

Summary of Data Requirements

The model operates with the following data sets:

Climotological Data

On a daily basis for a period of 1 year:

1. Maximum air temperature
2. Minimum air temperature
3. Average relative humidity
4. Total precipitation
5. Solar radiation

Dump Geometry Data

1. Gradient
2. Slope length
3. Slope aspect

Soil Data

1. Mean size diameter of slope soil
2. Density of slope soil

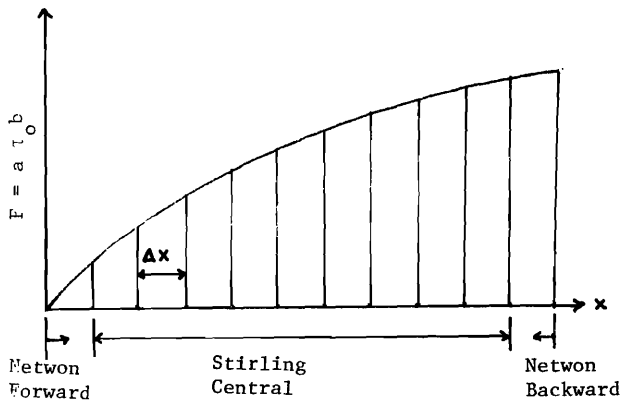


Fig. 3.8. Numerical integration stratagem

RESULTS

Soil Erosion

Computer model

The computer model developed as part of this study generates the amount of soil loss, in pounds per unit width, based on the site, climate, topography and soil parameters. The climatic portion of the model generates a flowrate (cfs/ft from snowmelt or rainfall) which is used by the erosion simulation portion of the model together with the slope length, gradient and soil parameters to compute the amount of erosion. The theoretical framework for the mathematical erosion model is described in Chapter 3 (Methodology) of this report and a listing of the computer program is provided in Appendix A.

Field data

Field erosion data are obtained from a study by the Forestry Sciences Laboratory on the U.S.U. campus. The Forestry Sciences study collected sediment and total runoff in tanks from plots at the Wooley Valley mine in Southeastern Idaho. The Forestry Sciences, F. S., erosion plots are approximately 76 ft. in length and are constructed at a slope of 3 horizontal to 1 vertical (see Appendix B for details). The F. S. erosion plots are constructed such that the sediment laden runoff is trapped at the downstream end of slope. The measurement of sediment and total volume of water, in the catchments basins, were taken about 5 to 6 times a year. The amount of soil loss and the total depth of runoff (the volume of water in the catchment basin

divided by the area of the erosion plot), from bare soil plots, display no consistent relationship (Figure 4.1). The almost random distribution of data in Figure 4.1 perhaps indicates the extreme variability in the erosion characteristics which is very difficult, if not impossible, to explain mathematically. One can only speculate the conditions that could have caused the wide scatter of these data. The affect of vegetation, arrangement of rocks in slope surface, response to freezing and thawing cycles, formation of rills and gullies, interference from adjoining plots, soil moisture conditions through time and disturbance by human or animal treading on the erosion plots have to be taken in account in order to explain the variability of this erosion data. The mathematical model developed in this study cannot be used to explain the response to these factors. Hence, to abstract away from the variability in the data it is assumed that the daily soil loss varies linearly with the total daily runoff. The total average measured soil loss over the two year period (1976 and 1977) is then distributed according to the amount of daily runoff;

$$E_{mi} = E_{mT} \frac{d_i}{d_T} \dots \dots \dots (4.1)$$

where

- E_{mi} = daily soil loss (lb/ft)
- E_{mT} = total measured soil loss over the two year study period
- d_i = depth of daily runoff
- d_T = total depth of runoff over the two year study period

The results produced by Eq. 4.1 are then used to calibrate the model with field data. This type of approach in using the field data to calibrate the computer model implies that model would not yield good results for a single storm, but when used over a long period (water year) the result would be better.

Calibration of model with field data

Daily soil loss, at the F. S. erosion plots (slope length = 76', gradient = 33%), is computed using the computer model developed herein in conjunction with the 2 years of climatic data and soil parameters at the phosphate mine sites in Southeastern Idaho. The results produced by Eq. 4.1 are plotted against the daily erosion computed by the computer model (Figure 4.2). The best fit straight line, forced through the origin, through these data displays the following form:

$$E_m = 6.283 \times 10^{-7} E_{AW} \quad (4.2)$$

$$R^2 = 0.9878$$

where

E_m = normalized measured erosion per unit width of slope (lb/ft)

E_{AW} = amount of erosion per unit width computed by model (lb/ft)

R^2 = correlation coefficient

Eq. 4.2 indicates the calibration coefficient which, when applied to the results produced by the computer model, yields the measured amount of erosion.

Affect of flowrate and slope length

To investigate the influence of variable slope length and flow rate on soil loss, simulations were obtained using the erosion portion of the model. The flowrate is calculated according to Eq. 3.37 and 3.38 using a time duration of 2 hours. The slope is maintained constant at 3 horizontal and 1 vertical.

Volumetric erosion rate. Using 3 storm sizes and 4 different slope lengths, the volumetric erosion rates per unit width (ft³/ft-sec) computed by the model are summarized in Table 4.1.

$$E_{VL} = C_f 1.52 q^{0.932} SL^{0.296} \quad (4.4)$$

$$R^2 = 0.9925$$

where

E_{VL} = the volumetric erosion rate per unit width of slope

Since $P = 2$ is used in the equation of motion for sediment transport (Eq. 3.6) the mean size diameter of the slope material (D) and specific gravity (Sg) can be factored out of Eq. 4.4. The mean size diameter of the soils at the phosphate mine site in Southeastern Idaho is 0.0039 ft (1.19 mm) and $Sg = 2.72$, hence, in general the volumetric erosion can be expressed as:

$$E_{VL} = \frac{C_f 0.01754}{D(Sg - 1)^2} q^{0.932} SL^{0.296} \quad (4.5)$$

Rate of erosion. Multiplying the volumetric erosion rate by the dry unit weight of soil yields the rate of soil erosion per unit width of slope. For a slope of 3 horizontal to 1 vertical, this equation is:

$$E_{RL} = C_f \frac{0.01754 \gamma_d}{D(Sg - 1)^2} q^{0.932} SL^{0.296} \quad (4.6)$$

where

E_{RL} = rate of erosion per unit width, on slope of 3 horizontal to 1 vertical (lb/ft-sec)

Table 4.1. Volumetric erosion rate as a function of storm size, slope length and flowrate for the soils at the phosphate mine sites in Southeastern Idaho (for a slope of 3 horizontal to 1 vertical).

Total depth of storm (inches)	Duration of storm (hours)	Slope length (ft) (SL)	Flowrate at the bottom of the slope (cfs/ft) (q)	Volumetric erosion rate (ft ³ /ft-sec) (E_v)
1.66	2.	76.	0.00262	0.02076
1.66	2.	100.	0.00344	0.03347
1.66	2.	200.	0.00689	0.06857
1.66	2.	300.	0.01033	0.11389
2.22	2.	76.	0.00349	0.02857
2.22	2.	100.	0.00495	0.03494
2.22	1.	200.	0.00918	0.09936
2.22	2.	300.	0.01377	0.14916
2.77	2.	76.	0.00437	0.03671
2.77	2.	100.	0.00574	0.04546
2.77	2.	200.	0.01148	0.11853
2.77	2.	300.	0.01722	0.18537

The erosion rate as a function of flowrate at the bottom of the slope and slope length for the soils at the phosphate mines is presented in Figure 4.3.

Amount of erosion. Since 1 acre-in. is approximately equal to 1 cfs-hr, the amount of erosion, in pounds per foot of slope can be expressed as:

$$E_M = \frac{22680.75 \gamma_d C_f t_d}{D(Sg - 1)^2} q^{0.932} SL^{0.296} \quad (4.7)$$

where

E_M = amount of erosion per unit width of slope (lb/ft)

C_f = calibration coefficient that relates model results to field observations (dimensionless)

t_d = time over which flow (from snowmelt or rainfall) occurs (hours)

For the soils at the phosphate mine sites in Southeastern Idaho, $\gamma_d = 95 \text{ lb/ft}^3$ and $D = 0.0039/\text{ft}$ (1.19 mm) and $S_g = 2.72$. Assuming that $C_f = 6.283 \times 10^{-7}$ (from Eq. 4.1) is valid for all slope lengths at a slope of 3 horizontal to 1 vertical, the amount of erosion per unit width at the phosphate mines can be expressed as:

$$E_2 = 117.33 t_d q^{0.932} SL^{0.296} \dots (4.7)$$

where

E_2 = soil loss, in pounds per foot of slope width, at the phosphate mine sites in Southeastern Idaho, from slopes of 3 horizontal to 1 vertical.

Summary of Results

The general equation for erosion per unit width for slope of 3 horizontal to 1 vertical can be expressed by Eq. 4.6, where C_f is a coefficient that must be developed on the basis of field erosion data in the following manner: Assume $C_f = 1$ and use Eq. 4.6 (or better the computer model in conjunction with necessary data (Appendix A)) to compute soil loss per unit width of slope. Then plot the field data versus the computed soil loss, the slope of the best fit straight line forced through the origin is then equal to C_f for the particular site. For the phosphate mine sites the erosion per unit width on a slope of 3 horizontal to 1 vertical can be expressed as Eq. 4.7.

The affect of slope on erosion has not been studied. A slope of 3 horizontal to 1 vertical has been maintained constant. However, this can be incorporated into the computer model with minor changes in the FORTRAN code.

DISCUSSION

Summary of This Study

The objective of this study was to develop a mathematical model which describes erosion based on the site climate, topography and soil parameters. The model developed herein has been implemented in the form of a computer program. The mathematical model is developed using the equations of motion and continuity for sediment transport, dynamic and continuity equations for spatially varied flow with lateral inflow and equations of boundary shear stress subject to overland flow. Several simulation solutions were obtained for the soils at the phosphate mine sites, in Southeastern Idaho, using the two years of climatic data

available there. The computer model is calibrated using field erosion data obtained from a study by the Forestry Sciences Laboratory on the U.S.U. campus. The slope has been maintained constant at 3 horizontal to 1 vertical, primarily because slope stability considerations for the other overburden spoil dumps at the phosphate mine sites dictate this (Riker, Anderson and Jeppson, 1978). However, variable slope can be incorporated into the model with minor changes in the FORTRAN code.

Relationship of Model Results To Field Data

A plot of the computed vs. measured soil loss, pounds per foot of slope width, is furnished in Figure 4.2. The measured soil loss is much smaller than that computed by the model (Eq. 4.1). This could be attributed to the assumptions made to simplify the mathematics of the erosion model and the lack of climatic data at the phosphate mine sites. Also, the field erosion data is not consistent with the total depth of runoff (Figure 4.1) indicating that there are other factors that influence erosion characteristics considerably. The approach used in utilizing the field data is to abstract away from these other factors (e.g. vegetative cover, soil moisture condition, influence of freezing and thawing cycles, affects of channelization, disturbances caused by trampling on the erosion plots, heterogeneity of soil, physiochemical properties of soil, etc.) and distribute the total observed soil loss on the basis of the total observed depth of runoff and daily runoff as indicated in Eq. 4.1. The affects of these other factors then shows up as coefficient as shown in Eq. 4.2.

Implications of Modeling Procedure

The assumptions made in implementing the mathematical model are described in Chapter 3 of this report.

Soil parameters

The equation of motion for sediment transport (Eq. 3.5) as used in this study employs only the mean size diameter and specific gravity of the slope material. The other soil parameter used in implementing the model is the dry unit weight of soil. This places some limitations on using the model for universal application, because it fails to account for plasticity, compaction of the slope and heterogeneous deposits. The assumptions made regarding the soil parameter were that the slope material was non-cohesive, loose and homogeneous. The soils at the phosphate mine sites, in Southeastern Idaho, display very little plasticity (Riker, Anderson and Jeppson, 1978), however, even a slight cohesion can influence erosion

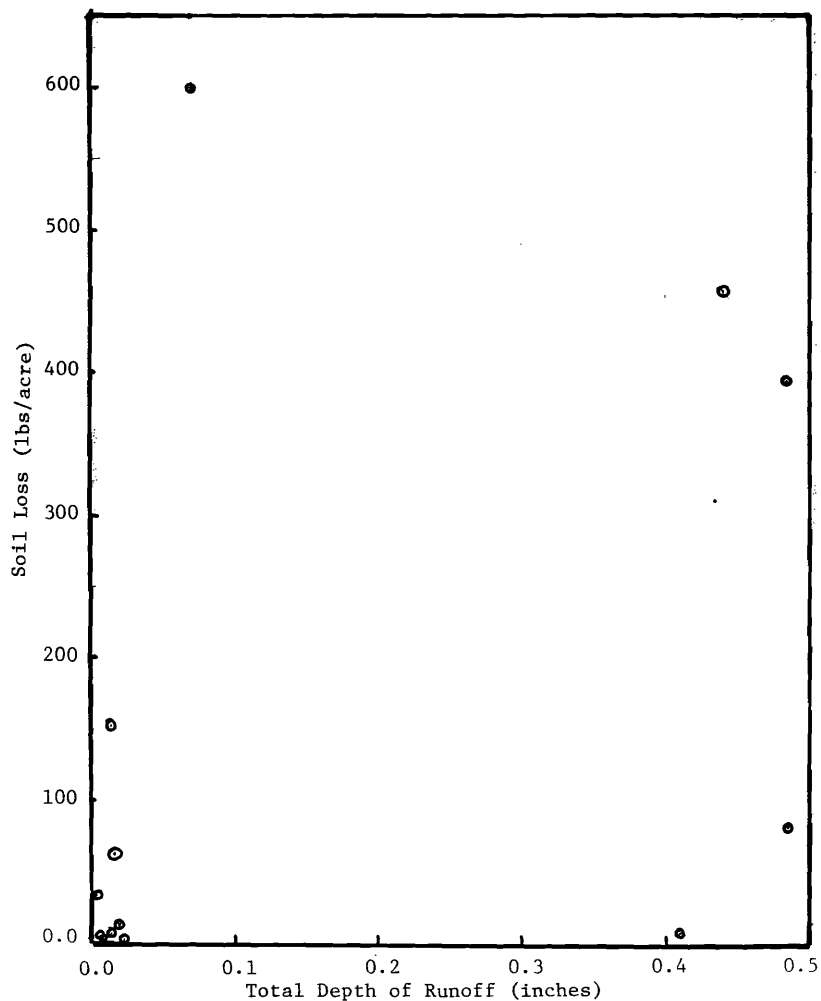


Fig. 4.1. Field erosion data from rare soil plots at the Wooley Valley Mine in S. E. Idaho.

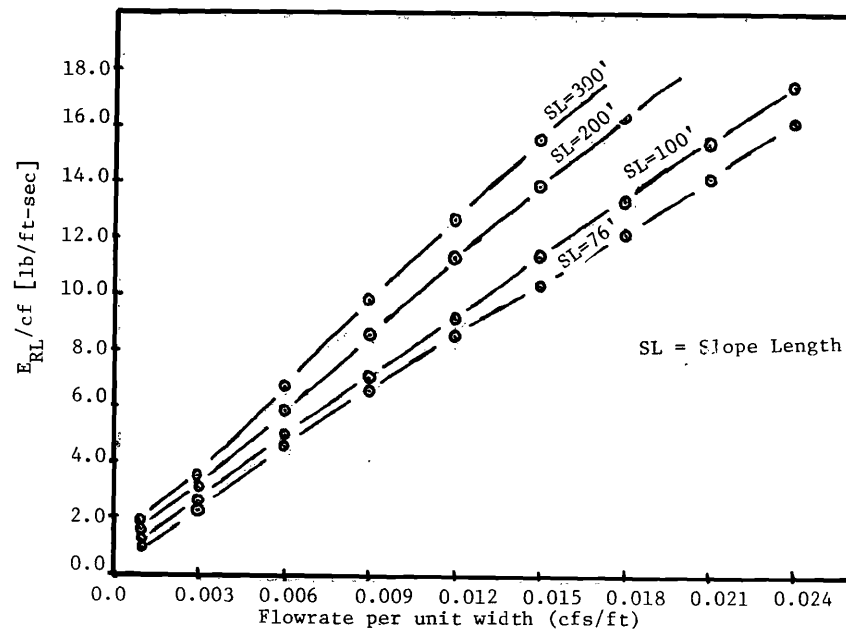


Fig. 4.3. Erosion rate per unit width over the calibration coefficient as a function of flowrate and slope length on a slope of 3 horizontal to 1 vertical for the soils at the phosphate mine sites in S. E. Idaho.

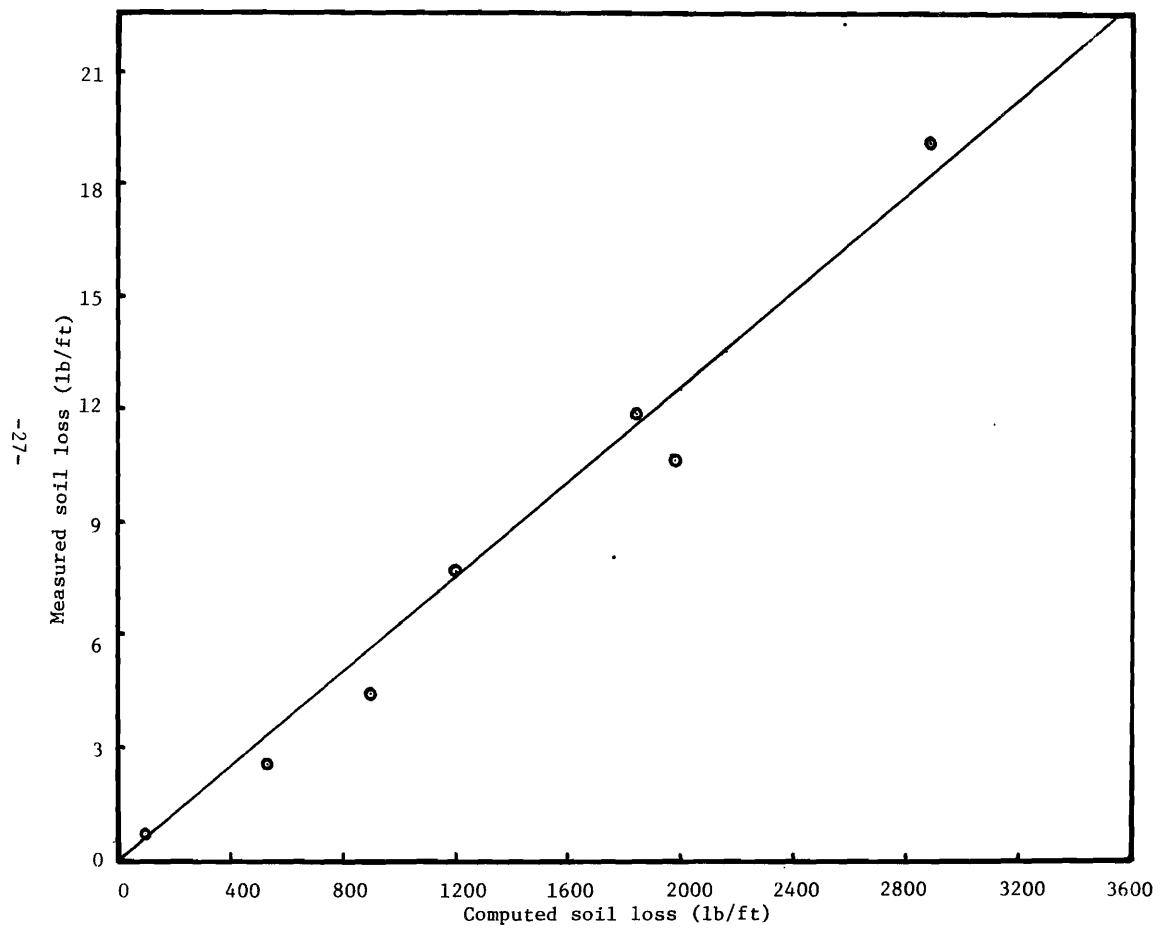


Fig. 4.2. Relationship of model results to field data

characteristics considerably and cause C_f to be quite different than that found for the F. S. plots. A soil parameter such as relative compaction or relative density should also be incorporated into the equation of motion and/or the equation of continuity for sediment transport. The assumption that the slope material is homogeneous could also lead to considerable errors in the model, since the material in the dumps is far from homogeneous (Riker, Anderson, and Jeppson, (1978). Rocks that lie embedded in the slope face could change the energy dissipation characteristics and, hence, the erosion characteristics of the slope. In addition, the soil moisture conditions through time and more comprehensive information and the infiltration rates could be incorporated into the model through runoff coefficients. The affect of freezing and thawing cycles on the erosion characteristics would be valuable information and could be used in the model, if available.

One-dimensional flow

While the assumption that the flow is one-dimensional may not be too far from the conditions in the field, it could have serious consequences on the results, for it ignores the channelization affect. The departure from sheet flow to flow in rills and gullies is a two-dimensional phenomena which occurs during the erosion process. The model developed as part of this study is valid only for sheet flow conditions. Komura (1976) suggests the following erodibility coefficients (Table 5.1). This implies that under erosion with rill there may be 5 times as much erosion and under erosion with gullies 10 times as much soil loss as that under purely sheet flow conditions.

Table 5.1. Erodibility coefficients for various types of erosion (after Komura, 1976).

Erosion Type	Erodibility Coefficient
sheet erosion	1.0
sheet erosion with small rills	1.0
sheet erosion with rills	5.0
sheet erosion with gullies	10.0

One way to handle channelization, and still use the simplicity of one-dimensional flow, might be to obtain the numerical solution to the water surface profile equation (Eq. 3.1) based on an equivalent flowrate q , which reflects the channelization affect. This could be accomplished in the following manner: Compute the total flowrate (ft^3/sec) that is occurring over the entire face of the dump, then to obtain the equivalent one-dimensional flow divide the total flowrate by the product of the width of the dump and a flow

concentration coefficient (less than 1.0). This flow concentration coefficient reflects the percentage of the area over which the flow actually occurs, so as to leave out the no-flow region of the dump face.

Data Limitations and Recommendations

Climatic data

At the present time there are no official weather stations at the phosphate mine sites in Southeastern Idaho. Good information about the daily weather, which includes temperature, humidity, precipitation, wind speed and solar radiation data, at the mine sites, is vital data for any erosion simulation study. In addition, measurements of snowmelt hydrographs should occur to facilitate and check the snowmelt predicted by the computer solution used in this study.

Erosion data

The erosion simulation model developed in this study computes the time rate of erosion per unit width. However, at the present time, there is no information on the rate of erosion in the field. These data could be developed using the existing facilities at the erosion plots at the Wooley Valley mine by measuring the volume of water and sediment that enters the catchment basins at some pre-decided time intervals. These measurements could be made during rainstorms and the spring snowmelt period to yield the time rate of soil erosion per unit width in the field. This information would greatly enhance the basic understanding of the mechanics of soil erosion. Also the availability of field erosion rates would facilitate a more realistic calibration of the model developed in this study.

Also, analysis of grain size distribution and other properties of the sediment, that is trapped in the catchment basins at the erosion plots, should be carried out. The relationship of the properties of sediment and the original soil could yield valuable insight about erosion mechanics.

Conclusions

The conclusions obtained from the results of this investigation are as follows:

1. The general equation of slope erosion for overburden spoil dumps at the phosphate mine sites in Southeastern Idaho can be expressed by Eq. 4.7, for a slope of 3 horizontal to 1 vertical.
2. The erosion model developed in this study,

due to calibration approach used, will not yield good results for a single storm or a day of snowmelt, but when used over a long period (a water year) the result will be much better.

3. The general equation of erosion on slopes of 3 horizontal to 1 vertical can be expressed as:

$$E_M = \frac{22680.75 \gamma_d C_f t_d}{D(Sg - 1)^2} q^{0.932} SL^{0.296}$$

where C_f is a calibration coefficient which must be solved for on the basis of field erosion data.

4. Additional studies are needed to incorporate slope into the calibration of the erosion model.

BIBLIOGRAPHY

- Allen, J. 1934. Streamliner and turbulent flows in open channels. Phil. Mag. 17:1081-1112.
- Anderson, H. W. 1951. Physical characteristics of soil related to erosion. J. of Soil and Water Conservation, July, pp. 129-133.
- Arulanandan, K., P. Loganathan and R. B. Krone. 1972. The influence of pore fluid composition on the erodibility of a soil. Univ. of California, Davis, Technical note, Sept.
- ASCE Task Committee on Erosion of Cohesive Materials. 1968. Erosion of cohesive sediments. Journal of the Hydraulic Division, ASCE, Proc. Paper 6044, July.
- Beer, C. E., C. W. Farharn and H. G. Heinemann. 1966. Evaluating sediment predication techniques in Western Iowa. Transaction of the A.S.A.E., 9(6):828-833.
- Berghager, D., and C. C. Ladd. 1964. Erosion of cohesive soils. Dept. of Civil Engineering, M.I.T., Research Report R64-1, January.
- Bolger, J. C., 1960. Rheology of Kaolin suspensions. ScD. Thesis, M.I.T.
- Carson, M. A. and M. J. Kirly. 1972. Hillslope form and process. Cambridge University Press, pp. 35-55.
- Chen, C. L. 1975. Urban storm runoff inlet hydrograph study. Vol. 2. PRWG106-2, Utah Water Research Laboratory, U.S.U., May.
- Chow, V. T. 1959. Open-channel hydraulics. McGraw-Hill Book Co., New York, N. Y. pp. 7-16, 179-188, 543-549.
- Conner, A. B., R. E. Dickson, and D. Scoates. 1930. Factors influencing runoff and soil erosion. Texas Ag. Exp. Sta. Col. Sta. Bull. No. 411, March.
- David, W. P. 1972. Digital simulation of sheet erosion. Unpublished Ph. D. thesis, Iowa State University of Science and Technology Library, Ames, Iowa.
- Dunn, I. S. 1959. Tractive resistance of cohesive channels. Proc. of the Am. Soc. of Civil Engr., Vol. 85, SM3, June.
- Ellison, W. D. 1947. Soil erosion studies - Part II, Soil detachment hazard by raindrop splash. Ag. Engr. Vol. 28, pp. 197-201.
- Ellison, W. D. 1944. Studies of raindrop splash. Ag. Engineering, Vol. 25, pp. 131-136, 181-182.
- Ellison, W. D. 1947. Soil erosion studies - Part VI, Soil detachment by surface flow. Ag. Engineering, Sept. pp. 402-408.
- Forrest, L.A., and J.F. Lutz. 1944. Slope and water reduction effecting the movement of soil properties - 2 Field Study. Soil Science Society, Proc., 9:17-23.
- Foster, R. L. and G. L. Martin. 1969. Effect of unit weight and slope on erosion. Jour. of the Irrigation and Drainage Division, Proc. ASCE, Vol. 95, No. IR4, December.
- Gottshalf, L. C. and G. M. Grune. 1950. Sediment design criteria for the Missouri Basin loess hills. U.S.D.A Soil Conservation Service Technical publication No. 97.
- Henderson, F. M., 1966. Open channel flow. McMillan Publishing Co., Inc., New York, N. Y. pp. 91.
- Hopf, L. 1910. Turbulenz bei einen flusse. Ann. Physik, 337, Vierte Folge, 32:777-808.
- Horton, R. E., H. R. Leach, and R. Van Vliet. 1934. Laminar sheet flow. Trans. Amer. Geophys. Union, 15:393-404.
- Jeffreys, H. 1925. The flow of water in an inclined channel of rectangular section. Phil. mag., 49:292, 793-807.
- Jeppson, R. W., R. W. Hill and E. C. Israelsen. 1974. Slope stability of overburden spoil dumps from surface phosphate mines in southeastern Idaho. PRWG 140-1, Utah Water Research Laboratory, U.S.U., April.
- Komura, S. 1976. Hydraulics of slope erosion. J. of the Hydraulic Division, Proc. ASCE, Vol. 102, No. HY10, Oct.
- Lane, E. W. 1955. Design of stable channels. Trans. of the Am. Soc. of Civil Engr., Vol. 120.
- Li, R. M., H. W. Shen and D. B. Simons. 1973. Mechanics of soil erosion by overland flow. Proceedings of the 15th Congress, International Association of Hydraulic Research, Istanbul, Turkey, Vol. 1, Spet. pp. 437-446.
- McIntyre, D. S. 1958. Soil splash and the formation of surface crusts by raindrop impact. Soil Sci., Vol. 85, pp. 261-266.

- Meyer, L. D., and E. J. Monke. 1965. Mechanics of soil erosion by rainfall and overland flow. Trans. A.S.A.E., Vol. 8, pp. 572-577, 580.
- Musgrave, C. W. 1947. Qualitative evaluation of factors in water erosion--a first approximation. Jour. Soil and Water Conservation 2(3):133-138.
- Nichols, M.D. 1936. Technology of erosion control. Soil Science Society, Proc., 1:393-399.
- Osborn, Ben. 1954. The theory of infiltration - IV, Sorptivity and algebraic infiltration equations. Soil Science, Vol. 84, pp. 257-264.
- Odborn, B. 1955. How rainfall and runoff erode soil. USDA Yearbook.
- Rose, C. W. 1960. Soil detachment caused by rainfall, Soil Science, Vol. 89. pp. 28-35.
- Rouse, H. 1959. Engineering Hydraulics. John Wiley and Sons, Inc., New York, N. Y. p. 797.
- Smerdon, E. T. and R. P. Beasley. 1959. The tractive force theory applied to the stability of open channels in cohesive soils. Univ. of Missouri, Agricultural Exp. Station, Res. Bull. 715, Oct.
- Straub, L. E., E. Silberman, and H. C. Nelson. 1958. Open channel flow at small Reynolds numbers. Trans. Amer. Soc. Civil Engineers, 123:685-706.
- Smith, D. D. and W. H. Wischmeier. 1957. Factors affecting sheet and rill erosion. Trans. Am. Geophysical Union, Vol. 38, No. 6, pp. 889-896.
- Wischmeier, W. H. and D. D. Smith. 1958. Rainfall energy and its relation to soil loss. Trans. Am. Geophys. Union 39:285-291.
- Wischmeier, W. H. and D. D. Smith. 1965. Predicting rainfall erosion losses from cropland east of the Rocky Mountains. USDA Handbook, No. 282.
- Woo, D. S. and E. F. Brater. 1961. Laminar flow in rough rectangular channels. Jour. Geophys. Res., 66(12):4207-4217.

APPENDIX A

COMPUTER PROGRAM INPUT DATA REQUIREMENTS AND LISTING FOR EROSION SIMULATION

Table A-1. Erosion simulation model input data requirements

Card number and format.	Description of variables
FORTTRAN variables on this card (or cards)	
Card 1 (free format, i.e. numbers separated by commas)	
Time	time base by the snowmelt period.
Rlim	Limiting Reynolds number (when this is reached, computations will be based on laminar flow equations)
Qlim	Limiting flowrate value, i.e. for q's smaller than this no erosion simulation will be carried out.
Iuti	If Iuti = 1, numerical solution to the W.S.P. equation will be printed.
Step	Increment (ft) to be used in storing values in solution arrays, eg., a value at every foot along the slope length.
Iut2	If Iut2 = 1, erosion rate along the slope will not be output.
Iut3	Increment to be used to print erosion rates along the slope.
Card 2 (free format)	
NTEMPU	NTEMPU = 0, if temperature data is being read in °F. NTEMPU = 1, if temperature data is being read in °C.
CONS1	Constant to be applied to humidity data.
CONS2	Constant to be applied to windspeed data.

Card number and format	Description of variables
FORTTRAN variables on this card (or cards)	
SLH	Slope length on a horizontal face (with respect to solar radiation).
SLN	Slope length on a north facing slope.
SLW	Slope length on a west facing slope.
SH	Gradient on horizontal faced dump.
SN	Gradient on the north facing dump.
SW	Gradient on the west facing dump.
Card 3 (free format)	
ERR	Closure error criteria to be used in generating the numerical solution to the W.S.P. equation.
HH	Initial step size to be used in starting the numerical solution.
UW	Dry unit weight of soil.
Card 4 (13A3)	
XMD (13)	13 element array of 3 character month abbreviation for output of dates, i.e., AUGSEP --- JUL ANN. ANN must be the 13th abbreviation. Order of others must match order of subsequent data.
Card 5 (6I5)	
ITY,NN(S)	ITY is a control parameter for climate data = 0 program stops = 1 climate data input by day for entire 365 day period = 2 climate data input by days by month for 12 month period

Table A-1, Cont.

Card number and format.	Description of variables
FORTTRAN variables on this card (or cards)	
	NN is a 5 element array of integers greater than zero, i.e. (1,1,1,1,1)
Card 6 (12I5) (ID(12))	12 element array of the day of the month for which corresponding values of solar radiation (card 7) are available (in order as indicated by XMD)
Card 7 (12F5.0) RD(12)	Solar radiation for select days above
Card 8 (12I5) IR(12)	Same as ID above, only for radiation indices on following cards
Card 9 (12F5.1) RH(12)	Radiation indices on selected days each month of a 12 month period for horizontal surface at the latitude of the site
Card 10 (12F5.1) RW(12)	Same as above for west facing slope
Card 11 (12F5.1) RN(12)	Same as above for north facing slope
If ITY = 1 read the following cards (12 thru 16)	
Card 12 (6A6) (FMT(6))	Format with which following climate data on cards are read, eg, (16F5.0)
Card 13 (FMT) TA(365)	Daily average air temperature
Card 14 (FMT) H(365)	Daily average humidity (fraction)
Card 15 (FMT) P(365)	Daily total precipitation (inches)

Card number and format.	Description of variables
FORTTRAN variables on this card (or cards)	
Card 16 (FMT) V(365)	Daily average windspeed (m.p.h.)
If ITY = 2 card following cards (17 thru 26)	
Card 17 (6A6) FMT(6)	Format for TMX below
Card 18, as many as req'd, (FMT) TMX(365)	Daily maximum air temperature by day according to months (start a new month on a new card)
Card 19 (6A6) FMT(6)	Format for TMN below
Card 20, as many as req'd, (FMT) TMN(365)	Daily minimum air temperature by day according to months.
Card 21 (6A6) FMT(6)	Format for H below
Card 22, as many as req'd, (FMT) H(365)	Daily average humidity (traction)
Card 23 (6A6) FMT(6)	Format for P below
Card 24, as many as req'd, (FMT) P(365)	Daily total precipitation (inches)
Card 25 (6A)	Format for V below
Card 26, as many as req'd, (FMT) V(365)	Daily average windspeed (m.p.h.)

```

COMMON /ISOL/IUT3,HW
6(KIND=REMOTE,MAXRECSIZE=14)
5(KIND=DISK,TITLE=DATA,FILETYPE=7)
COMMON /EROS/HH,ERR,IUT1,IUT2,STEP
COMMON /FC/C,RLIM
DIMENSION V(365),TA(365),H(365),P(365),ES(365),RAD(365),RIH(365),
IRIN(365),RIW(365)
DIMENSION ID(12),RD(12),IR(12),RH(12),RW(12),RN(12)
DIMENSION NN(5),FMT(6),TMX(365),TMN(365)
DIMENSION MD(12),XMD(13)
DIMENSION TAV(13),TV(13),PAV(13),PV(13)
DATA MD/31,30,31,30,31,31,28,31,30,31,30,31/
30 REWIND 5
WRITE(6,1001)
31 FORMAT(2X,'ENTER TIME,RLIM,QLIM,IUT1; OR "END" ')
READ(5,/,END=991) TIME,RLIM,QLIM,IUT1,STEP,IUT2,IUT3
READ(5,/)TEMPU,CONS1,CONS2,SLH,SLN,SLW,SH,SN,SW
READ(5,/)ERR,HH,HW
UNITS=SLH/(12.*TIME)
VNITS=SLN/(12.*TIME)
WNITS=SLW/(12.*TIME)
QN=0.0
QH=0.0
QW=0.0
READ(5,105) XMD
READ(5,130) ITY,NN
32 FORMAT(13A3)
IF(ITY.LE.0) STOP
READ(5,130) ID
READ(5,131) RD
READ(5,130) IR
READ(5,133) RH
READ(5,133) RW
READ(5,133) RN
33 FORMAT(12I5)
1 FORMAT(12F5.0)
2 FORMAT(/20X'MONTH OF 'A3/4(3X'DAY RAD RIH RIW RIN')/)
3 FORMAT(12F5.1)
4 FORMAT(4(I6,4F6.1))
IF(ITY.EQ.2) GO TO 60
READ(5,135) FMT
34 FORMAT(6A6)
READ(5,FMT) TA
READ(5,FMT) H
READ(5,FMT) P
READ(5,FMT) V
GO TO 30
35 DO 70 L=1,5
IF(NN(L).LE.0) GO TO 70
READ(5,135) FMT
MI=1
DO 68 MM=1,12
MF=MI+MD(MM)-1
GO TO(61,62,63,64,65),L
1 READ(5,FMT)(TMX(J),J=MI,MF)
IF(NTMPU.EQ.0) GO TO 66
DO 211 J=MI,MF
1 TMX(J)=32.+TMX(J)*1.8
GO TO 66
2 READ(5,FMT)(TMN(J),J=MI,MF)
IF(NTMPU.EQ.0) GO TO 66
DO 311 J=MI,MF

```

```

11 TMX(J)=32.+TMX(J)*1.8
GO TO 66
53 READ(5,FMT)( H(J),J=MI,MF)
DO 511 J=MI,MF
11 H(J)=H(J)*CONS1
GO TO 66
54 READ(5,FMT)( P(J),J=MI,MF)
GO TO 66
55 READ(5,FMT)( V(J),J=MI,MF)
DO 411 J=MI,MF
11 V(J)=V(J)*CONS2
56 MI=MF+1
58 CONTINUE
70 CONTINUE
DO 75 J=1,365
75 TA(J)=(TMX(J)+TMN(J))*0.5
30 CONTINUE
MSD=0
NXT=1
LST=0
DO 50 J=1,365
MK=(J/(MSD+1))+LST
IF(MK.NE.NXT) GO TO 30
LST=NXT
NXT=NXT+1
MSD=MSD+MD(LST)
REMOVE THE C IN COLUMN ONE OF THE FOLLOWING CARD FOR DEBUG
WRITE(6,132) XMD(LST)
JJ=J
JP=JJ+MD(LST)-1
30 CONTINUE
L=J-MSD+MD(LST)
INTERPOLATE FOR RADIATION
IF(L.LT.ID(LST)) GO TO 33
MB=LST
ME=NXT
IF(ME.GE.13) ME=1
DS=L-ID(MB)
GO TO 35
33 MB=LST-1
ME=LST
IF(MB.LE.0) MB=12
DS=L+MD(MB)-ID(MB)
35 TDS=MD(MB)-ID(MB)+ID(ME)
RAD(J)=RD(MB)+(RD(ME)-RD(MB))*DS/TDS
IF(L.LT.IR(LST)) GO TO 43
MB=LST
ME=NXT
IF(ME.GE.13) ME=1
DS=L-IR(MB)
GO TO 45
43 MB=LST-1
ME=LST
IF(MB.LE.0) MB=12
DS=L+MD(MB)-IR(MB)
45 TDS=MD(MB)-IR(MB)+IR(ME)
RIH(J)=RH(MB)+(RH(ME)-RH(MB))*DS/TDS
RIW(J)=RW(MB)+(RW(ME)-RW(MB))*DS/TDS
RIN(J)=RN(MB)+(RN(ME)-RN(MB))*DS/TDS
IF(L.EQ.MD(LST))JP=J
IF(J.NE.JP) GO TO 50

```

```

REMOVE THE C IN COLUMN ONE OF THE FOLLOWING CARD FOR DEBUG
WRITE(6,134) (K,RAD(K),RIH(K),RIW(K),RIN(K),K=JJ,JP)
1) CONTINUE
C=0.0002
QT=1.0
B=0.0005
CK=0.0001
SNOW=0.0
SNWH=0.0
SNWN=0.0
SNWW=0.0
SMXH=1.0
SMXN=1.0
SMXW=1.0
HRS=10.
TLSP=0.0
PLSP=1.0
N=365
MSD=0
NXT=1
LST=0
DO 1 J=1,N
MK=(J/(MSD+1))+LST
IF(MK.NE.NXT) GO TO 20
LST=NXT
NXT=NXT+1
MSD=MSD+MD(LST)
TV(LST)=0.0
TAV(LST)=0.0
PV(LST)=0.0
PAV(LST)=0.0
20 CONTINUE
TB=TA(J)-TLSP
R=P(J)*PLSP
COMPUTE MONTHLY AVERAGES AND TOTALS
PV(LST)=PV(LST)+P(J)
PAV(LST)=PAV(LST)+R
TV(LST)=TV(LST)+TA(J)/MD(LST)
TAV(LST)=TAV(LST)+TB/MD(LST)
TX=TB-32.0
IF(TX.LT.0.0) TX=0.0
ES(J)=6.11+TX*(0.2+TX*0.008)
14 EA=H(J)+ES(J)
SNOW=0.0
QT=1.0
IF(TB.GT.32.0) GO TO 2
QT=2.0-TB/32.0
EVP=HRS*CK*V(J)*(EA-ES(J))/QT
EVP=-EVP
SNOW=R
SNWH=SNWH+SNOW
SNWN=SNWN+SNOW
SNWW=SNWW+SNOW
IF(SNOW.LE.0.0) GO TO 81
SMXH=SNWH
SMXN=SNWN
SMXW=SNWW
31 CONTINUE
SMCV=0.0
SMCD=0.0
GO TO 3

```

```

2 CONTINUE
EVP=0.0
SMCV=HRS*C*V(J)*(TB-32.0)/QT
SMCD=HRS*B*V(J)*(EA-6.11)/QT
IF(SMCD.LT.0.0) SMCD=0.0
3 CONTINUE
SNWH=SNWH-EVP
SNWN=SNWN-EVP
SNWW=SNWW-EVP
IF(SNWH.LT.0.0) SNWH=0.0
IF(SNWN.LT.0.0) SNWN=0.0
IF(SNWW.LT.0.0) SNWW=0.0
ALH=1.0-(0.20+0.80*SNWH/SMXH)
ALN=1.0-(0.20+0.80*SNWN/SMXN)
ALW=1.0-(0.20+0.80*SNWW/SMXW)
HHH=RAD(J)
HMN=RAD(J)*RIN(J)/RIH(J)
HMW=RAD(J)*RIW(J)/RIH(J)
SMRDH=ALH*HHH/(203.2*QT)
SMRDN=ALN*HMN/(203.2*QT)
SMRDW=ALW*HMW/(203.2*QT)
SMCALH=SMCV+SMCD+SMRDH
SMCALN=SMCV+SMCD+SMRDN
SMCALW=SMCV+SMCD+SMRDW
IF(SMCALH.GT.SNWH) GO TO 4
SMACTH=SMCALH
9 CONTINUE
IF(SMCALN.GT.SNWN) GO TO 5
SMACTN=SMCALN
10 CONTINUE
IF(SMCALW.GT.SNWW) GO TO 6
SMACTW=SMCALW
GO TO 8
4 CONTINUE
SMACTH=SNWH
GO TO 9
5 CONTINUE
SMACTN=SNWN
GO TO 10
6 CONTINUE
SMACTW=SNWW
8 CONTINUE
L=J-MSD+MD(LST)
RMACTH=SMACTH*UNITS
RMACTN=SMACTN*VNITS
RMACTW=SMACTW*WNITS
QH=QH+RMACTH
QN=QN+RMACTN
QW=QW+RMACTW
IF(TA(J).GT.32.0.AND.P(J).GT.0.0) GO TO 992
GO TO 993
992 QH=QH+P(J)*UNITS
QN=QN+P(J)*VNITS
QW=QW+P(J)*WNITS
993 IF(QH.GE.QLIM) GO TO 994
GO TO 995
994 CALL SNUMER(QH,SH,SLH)
QH=0.0
995 IF(QN.GE.QLIM) GO TO 996
GO TO 997
996 CALL SNUMER(QN,SN,SLN)

```

```

QN=0.0
07 IF(QN.GE.QLIM) GO TO 998
GO TO 999
08 CALL SNUMER(QN,SW,SLW)
QN=0.0
09 SNWH=SNWH-SMACTH
SNWN=SNWN-SMACTN
SNWW=SNWW-SMACTW
1 CONTINUE
GO TO 200
01 STOP
END
SUBROUTINE SNUMER(Q,SO,SL)
COMMON /EROS/HH,ERR,IUT1,IUT2,STEP
COMMON /ROS/A1,SLL,500
COMMON /SOLPT/NPOINT
REAL X(50),Y(50),DY(50)
REAL XX(200),YY(200),D(200),FS(200)
A1=Q
SLL=SL
500=SO
SIZE=-1.*STEP
WRITE(6,210)Q,SL,SO
210 FORMAT(1X,10X,'FLOWRATE= ',F10.8,'CFS/FT',5X,'/',10X,'SLOPELENGTH= ',
F10.5,'FT.',F10.8,'/',10X,'SLOPE= ',F10.8,'/')
Y(1)=UBOUND(Q)
X(1)=SL
I1=2
II=1
XX(I1)=X(1)
XN=1.0
H=HH
E=ERR
2 J=1
CALL SLOPE(J,X(J),Y(J),DY,SF)
FX=XX(I1)-X(J)
IF(FX.LT.0.0.AND.FX.GT.SIZE)II=II-1
IFX=FX/STEP
II=IFX+II
IF(II.EQ.I1) GO TO 101
XX(II)=X(J)
YY(II)=Y(J)
FS(II)=SF
II=II

```

```

101 X1=X(J)
DO 16 J=2,4
DY1=H*DY(J-1)
X(J)=X(J-1)+H/3.
Y(J)=Y(J-1)+(DY1/3.)
CALL SLOPE(J,X(J),Y(J),DY,SF)
DY2=H*DY(J)
X(J)=X(J-1)+(2.*H)/3.
Y(J)=Y(J-1)+(DY2-(DY1)/3.)
CALL SLOPE(J,X(J),Y(J),DY,SF)
DY3=H*DY(J)
X(J)=X(J-1)+H
Y(J)=Y(J-1)+DY3-DY2+DY1
CALL SLOPE(J,X(J),Y(J),DY,SF)
DY4=H*DY(J)
Y(J)=Y(J-1)+(DY1+3.*DY2+3.*DY3+DY4)/8.
FX=XX(II)-X(J)
IF(FX.LT.0.0.AND.FX.GT.SIZE)II=II-1
IFX=FX/STEP
II=IFX+II
IF(II.EQ.I1) GO TO 102
XX(II)=X(J)
YY(II)=Y(J)
FS(II)=SF
II=II
102 X1=X(J)
11 IF(H) 12,1,13
12 IF(X(J)-XN) 1,1,16
13 IF(X(J)-XN) 16,1,1
16 CONTINUE
J=4
PC=(Y(4)-Y(1)-(3.*H*(DY(4)+3.*DY(3)+3.*DY(2)+DY(1)))/8.)*242./27.
IF(ABS(H).LE.0.001) GO TO 600
IF(ABS(PC)-E) 19,19,45
19 M=1
20 J=J+1
Y(J)=Y(J-4)+(4.*H*(2.*DY(J-1)-DY(J-2)+2.*DY(J-3)))/3.
Y(J)=Y(J)-112.*PC/121.
X(J)=X(J-1)+H
CALL SLOPE(J,X(J),Y(J),DY,SF)
P=Y(J)
Y(J)=(9.*Y(J-1)-Y(J-3)+3.*H*(DY(J)+2.*DY(J-1)-DY(J-2)))/9.
PC=P-Y(J)
IF(ABS(PC)-E) 30,30,25
25 IF(H) 40,40,45
30 Y(J)=Y(J)+9.*PC/121.
M=0
CALL SLOPE(J,X(J),Y(J),DY,SF)
FX=XX(II)-X(J)
IF(FX.LT.0.0.AND.FX.GT.SIZE)II=II-1
IFX=FX/STEP
II=IFX+II
IF(II.EQ.I1) GO TO 103
XX(II)=X(J)
YY(II)=Y(J)
FS(II)=SF
II=II
103 X1=X(J)
31 IF(H) 33,1,34
33 IF(X(J)-XN) 1,1,35
34 IF(X(J)-XN) 35,1,1

```

```

35 IF(J-7) 20,36,36
   IF(ABS(H).LE.0.001) GO TO 600
36 IF(ABS(PC)-E/32.) 50,50,37
37 DO 38 J=1,6
   X(J)=X(J+1)
   Y(J)=Y(J+1)
38 DY(J)=DY(J+1)
   J=6
   GO TO 20
40 H=H/2.
   Y(1)=Y(J-1)
   X(1)=X(J-1)
   GO TO 2
45 H=H/2.
   GO TO 2
50 H=2.*H
   DO 55 J=2,4
   L=2*J-1
   X(J)=X(L)
   Y(J)=Y(L)
55 DY(J)=DY(L)
   J=4
   GO TO 20
1  X9=X(1)
30 NPOINT=II
   IF(IUT1.NE.1) WRITE(6,220)
20 FORMAT(1X,10X,'THE NUMERICAL SOLUTION TO THE W.S.P. EQUATION ',//)
   DO 104 II=1,NPOINT
   IF(XX(II).LE.0.0) XX(II)=XX(II-1)-STEP
   IF(FS(II).LE.0.0) FS(II)=FS(II-1)
   IF(YY(II).LE.0.0) YY(II)=2.*YY(II-1)-YY(II-2)
34 CONTINUE
   NPOINT=NPOINT+1
   XX(NPOINT)=0.0
   YY(NPOINT)=0.0
   FS(NPOINT)=0.0
   DX=XX(1)-XX(2)
   DX=-1.*DX
   IF(DX.EQ.0.0) DX=STEP
   DE=3.*YY(2)-11.*YY(1)/6.-1.5*YY(3)+YY(4)/3.
   D(1)=DE/DX
   DX=XX(2)-XX(3)
   IF(DX.EQ.0.0) DX=STEP
   DE=YY(3)-YY(1)/3.-0.5*YY(2)-YY(4)/6.
   D(2)=DE/DX
   NP=NPOINT-2
   DO 111 I=3,NP
   DX=XX(I)-XX(I+1)
   IF(DX.EQ.0.0) DX=STEP
   DE=2.*(YY(I+1)-YY(I-1))/3.-(YY(I+2)-YY(I-2))/12.
111 D(I)=DE/DX
   N=NPOINT
   DX=XX(N-1)-XX(N)
   IF(DX.EQ.0.0) DX=STEP
   DE=YY(N+1)/3.+YY(N)/2.-YY(N-1)+YY(N-2)
   D(N)=DE/DX
   N=N+1
   DX=XX(N-1)-XX(N)
   IF(DX.EQ.0.0) DX=STEP
   D(N)=DE/DX
   DE=11.*YY(N)/6.-3.*YY(N-1)+1.5*YY(N-2)-YY(N-3)/3.

```

```

   IF(IUT1.EQ.1) GO TO 106
   DO 105 II=1,NPOINT,IUT2
105 WRITE(6,200) XX(II),YY(II),D(II),FS(II)
200 FORMAT(3H X=F13.5,3X,2HY=E15.8,3X,6HDY/DX=E15.8,3X,2HS=F10.6)
106 CALL TURNER(XX,YY,D,FS)
   RETURN
   END
   FUNCTION BOUND(Q)
   B=0.13
   IF(Q.GE.0.01.AND.Q.LT.0.07) D=0.41962*Q**0.5269
   IF(Q.GE.0.0085.AND.Q.LT.0.01) D=0.3614*Q**0.49316
   IF(Q.GE.0.0071.AND.Q.LT.0.0085) D=0.34097*Q**0.48101
   IF(Q.GE.0.0055.AND.Q.LT.0.0071) D=0.30589*Q**0.4590
   IF(Q.GE.0.0039.AND.Q.LT.0.0055) D=0.24077*Q**0.41348
   IF(Q.GE.0.0028.AND.Q.LT.0.0039) D=0.08672*Q**0.23053
   M=0
   A=0.1641*Q**0.683
1 DD=0**1.5
   T1=0.10792*Q/DD-1.74
   T2=(D-A)/(B*D)+0.0000246/DD
   F=T1+2.*ALOG10(T2)
   T3=-0.16188*Q/(DD*D)
   T4=0.86859/T2
   T5=A/(B*D*D)-0.0000369/(DD*D)
   DF=T3+T4*T5
   ET=F/DF
   D=D-ET
   IF(D.LT.0.0) D=-1.*D
   M=M+1
   AET=ABS(ET)
   IF(AET.GT.0.00001.AND.M.LT.50) GO TO 1
   BOUND=D
   RETURN
   END
   SUBROUTINE SLOPE(J,X,Y,DY,SF)
   COMMON /RQS/A1,SLL,S00
   REAL DY(50)
   S0=S00
   QT=A1/SLL
   Q=QT*X
   G=32.2
   T3=2.*QT*Q/(G*Y*Y)
   T5=Q*Q/(G*Y*Y*Y)
   TH=.32175
   SF=FSLOPE(Y,Q)
   DY(J)=(S0-SF-T3)/(COS(TH)-T5)
   RETURN
   END
   FUNCTION FSLOPE(Y,Q)
   COMMON /FC/RLIM
   SET OWN
   REAL ET,III
   RESET OWN
   RE=Q/0.00001217
   IF(RE.LT.RLIM.AND. III.GE.5000.) GO TO 2
   M=0
   A=0.1641*Q**0.683
   B=.13
   R=(Y-A)/(B*Y)
   S=0.00022758/Q
   Z=0.395972*Q**0.208788

```



```

1 T1=R+S*Z
  F=Z-1.74+2.*ALOG10(T1)
  DF=1.+0.86859*S/T1
  IF(DF.EQ.0.0) DF=5.87107
  E=F/DF
  Z=Z-E
  M=M+1
  IF(ABS(E).GT.0.001.AND.M.LT.25) GO TO 1
  FF=(1./Z)**2.
  IF(RE.GE.RLIM) GO TO 3
  IF(III.GE.5000.) GO TO 2
  III=5000.
  ET=FF*RE
  WRITE(6,10) ET
10 FORMAT(2X,'CONSTANT= ',F10.2)
2 FF=ET/RE
3 FSLOPE=Q*Q*FF/(257.6*Y*Y)
  RETURN
END
SUBROUTINE SINTG(K,P,X)
  REAL P(200),X(200),E(200)
  COMMON /ISUL/IUT3,UW
  DX=X(2)-X(1)
  DX=DX*UW
  E(2)=DX*(.375*P(1)+19.*P(2)/24.-5.*P(3)/24.+P(4)/24.)
  J=K-1
  DO 1 I=3,J
    DX=X(I+1)-X(I)
    DX=DX*UW
1  E(I)=E(I-1)+DX*((P(I-1)+P(I))*13./24.-(P(I-2)+P(I+1))/24.)
    DX=X(K)-X(J)
    DX=DX*UW
    E(K)=E(J)+DX*(3.*P(K)/8.+19.*P(J)/20.-5.*P(K-2)/24.+P(K-3)/24.)
    WRITE(6,30)
30 FORMAT(2X,18X,'EROSION RATE',24X,'X=FT',/,20X,'-----',24X,
  $'-----',/)
  DO 2 I=2,K,IUT3
2  WRITE(6,10) E(I),X(I)
10 FORMAT(1H ,10X,'(E20.3,10X))
  ER=E(K)/X(K)
  WRITE(6,20) E(K),ER
20 FORMAT(2X,5X,'THE TOTAL EROSION PER UNIT WIDTH= ',E20.5,/,5X,'ERO
  $SION PER UNIT AREA PER UNIT TIME = ',E20.5)
  WRITE(6,40)
40 FORMAT(1X,10X,'THE UNITS ARE LBS./SQ.FT.SEC. FOR THE EROSION RATE
  $',/)
  RETURN
END
SUBROUTINE TURNER(XX,Y,D,F)
  COMMON /SOLPT/NPOINT
  REAL D(200)
  REAL XX(200),Y(200),F(200),P(200),PP(200),X(200)
  NP=NPOINT
  SUM=0.0
  DO 1 I=1,NP
1  SUM=SUM+F(I)
  ANP=FLJAT(NP)
  SFR=SUM/ANP
  DO 2 I=1,NP
2  DE=ABS(D(I))
  I=62.4*F(I)*Y(I)

```

```

DT=62.4*SF3*DE
TEMP=0.41742*DT
T=ABS(T)
2 P(I)=TEMP*I**1.5
  MP=NP
  NPI=NP-1
  DO 3 I=1,NPI
  PP(MP)=P(I)
  X(MP)=XX(I)
3 MP=MP-1
  PP(1)=0.0
  X(1)=0.0
  K=NPOINT
  CALL SINTG(K,PP,X)
  RETURN
END

```

APPENDIX B

Table B1. A summary of erosion data collected
by F. S. study for 1976

Date Collected	May 1976 (snowmelt)		June 23rd 1976		July 27th 1976		August 8th 1976		Sept. 9th 1976	
Plot	Runoff (inches)	Soil loss lb/acre	Runoff (inches)	Soil loss lb/acre	Runoff (inches)	Soil loss lb/acre	Runoff (inches)	Soil loss lb/acre	Runoff (inches)	Soil loss lb/acre
S*-11	0.313	8.13	0.030	0.87	0.008	1.67	0.004	0.117	0.017	2.0
S -10	0.550	47.81	0.016	1.88	0.012	4.50	0.008	0.685	0.024	6.88
S -9	0.482	102.94	0.021	4.72	0.021	21.67	0.003	3.82	0.042	55.0
S -8	0.546	59.00	0.020	3.62	0.008	5.37	0.004	0.616	0.024	7.5
S -7	0.554	16.56	0.012	1.81	0.008	2.19	0.002	0.205	0.016	1.88
S -6	0.363	110.95	0.023	3.58	0.010	6.05	0.003	0.692	0.02	12.11
S -5	0.493	109.61	0.021	4.72	0.012	4.39	0.003	0.365	0.014	10.56
S -4	0.294	61.59	0.015	3.18	0.011	13.47	0.004	0.516	0.015	22.35
S -3	0.424	8.19	0.012	2.81	0.012	12.69	0.004	0.822	0.024	8.75
S -2	0.428	27.85	0.022	2.50	0.011	3.90	0.003	1.260	0.025	5.0
S -1	0.428	158.55	0.013	2.55	0.013	5.50	0.003	0.515	0.019	11.0
T*-1	0.437	37.60	0.013	1.65	0.009	2.55	0.003	0.46	0.019	5.5
T -2	0.460	81.26	0.010	1.95	0.010	2.16	0.003	0.20	0.020	0.21
T -3	0.443	11.60	0.013	1.10	0.013	3.45	0.006	0.254	0.025	6.5
T -4	0.482	12.56	0.018	2.28	0.014	6.89	0.002	0.478	0.021	3.89
T -5	0.464	14.00	0.017	0.95	0.010	1.11	0.007	0.058	0.020	0.32
T -6	0.673	23.85	0.015	1.62	0.015	6.15	0.005	0.320	0.029	10.77
T -7	0.489	9.06	0.014	1.56	0.011	2.89	0.007	0.365	0.028	2.78
T -8	0.596	153.20	0.030	2.47	0.013	3.87	0.008	0.044	0.026	5.33
T -9	0.518	117.82	0.015	2.70	0.013	2.88	0.007	0.193	0.015	2.35
T -10	0.450	59.79	0.027	3.58	0.013	2.79	0.007	0.704	0.033	2.11
T -11	Tank Floated		-	-	-	-	-	-	-	-

* S = Spoils used on these plots

* T = Torsoil used on these plots

Table B2. A summary of erosion data collected
by F. S. study for 1977

Date Collected	May 27th 1977 (snowmelt)		June 13th 1977		July 11th 1977		Oct. 14th 1977	
Plot	Runoff (inches)	Soil loss lb/acre	Runoff (inches)	Soil loss lb/acre	Runoff (inches)	Soil loss lb/acre	Runoff (inches)	Soil loss lb/acre
S-11	0.57	349.0	0.004	32.0	0.013	29.0	0.017	1.0
S-10	0.24	209.0	0.002	1.0	0.016	12.0	0.024	2.6
S-9	0.48	457.0	0.007	1.0	0.042	83.0	0.042	3.6
S-8	0.51	144.0	0.002	1.0	0.016	7.0	0.020	1.1
S-7	0.38	37.0	0.002	1.0	0.008	2.0	0.016	0.6
S-6	0.41	387.0	0.010	2.0	0.013	12.0	0.023	0.6
S-5	0.28	143.0	0.005	2.0	0.014	14.0	0.021	1.7
S-4	0.07	600.0	0.007	3.0	0.015	20.0	0.018	1.9
S-3	0.55	433.0	0.008	2.0	0.008	8.0	0.016	0.6
S-2	0.44	38.0	0.014	4.0	0.009	5.0	0.009	1.0
S-1	0.44	38.0	0.009	1.0	0.009	7.0	0.013	1.0
T-1	0.39	12.0	0.013	1.0	0.019	5.0	0.022	1.0
T-2	0.39	10.0	0.007	1.0	0.010	5.0	0.016	1.0
T-3	0.42	7.0	0.009	1.0	0.013	5.0	0.025	0.6
T-4	0.44	10.0	0.007	1.0	0.014	4.0	0.017	0.5
T-5	0.43	1.0	0.007	1.0	0.010	1.0	0.02	0.5
T-6	0.55	6.0	0.005	1.0	0.015	4.0	0.024	1.0
T-7	0.01	3.0	0.014	1.0	0.007	1.0	0.028	0.7
T-8	0.57	81.0	0.013	5.0	0.013	3.0	0.025	1.3
T-9	0.52	115.0	0.007	3.0	0.011	5.0	0.015	1.2
T-10	0.47	3.0	0.020	1.0	0.013	5.0	0.02	0.5
¹ T-11	0.35	316.0	Tank Floated		0.18	16.75	0.038	6.8

¹ This plot is not reliable; the catchment tank floated from seepage pressures.

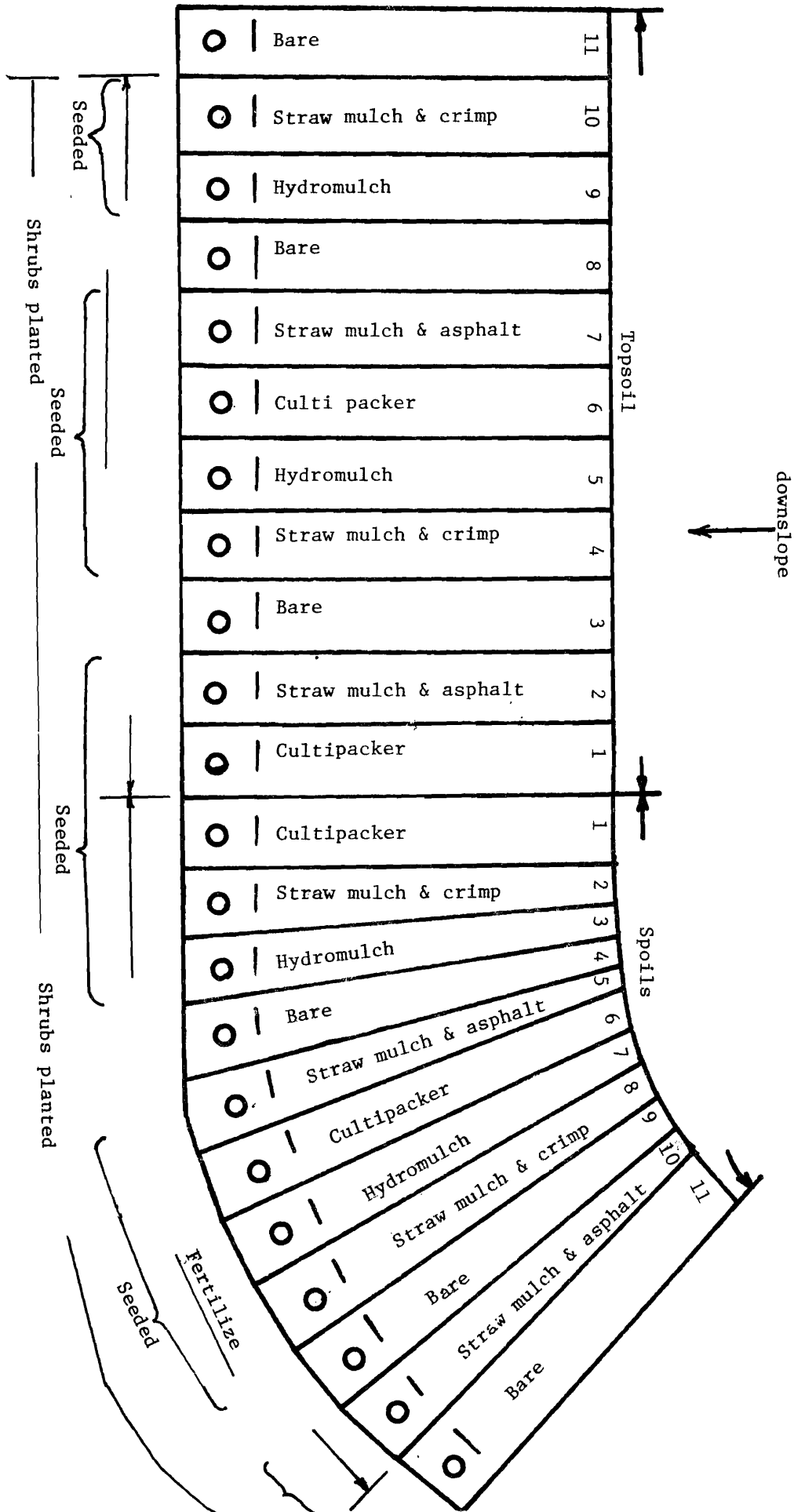


Fig. B1. Plane View of Woolley Valley Runoff and Erosion Plot Treatments

APPENDIX C

Table C1, Continued

Table C1. Daily flowrate (when $q > 0$), computed soil loss and the measure soil loss compared over the 2 year study period of available erosion data at the Wooley Valley erosion plots.

Flowrate, q at slope bottom	Computed soil loss (lb/ft ²)	Measured soil loss (lb/ft ²)	Flow rate, q at slope bottom	Computed soil loss (lb/ft ²)	Measured soil loss (lb/ft ²)
0.00003100	0.03265533	0.00063080	0.00004700	0.04812766	0.00095638
0.00012600	0.12065131	0.00256390	0.00001600	0.001763004	0.00032557
0.00022000	0.20282307	0.00447665	0.00012600	0.12065131	0.00256390
0.00001600	0.01763004	0.00032557	0.00028200	0.25562796	0.00573826
0.00003100	0.03265533	0.00063080	0.00054500	0.47237743	0.01108989
0.00001600	0.01763004	0.00032557	0.00039500	0.34994540	0.00803763
0.00001600	0.01763004	0.00032557	0.00063900	0.54788868	0.01300264
0.00001600	0.01763004	0.00032557	0.00003800	0.03947850	0.00077324
0.00001600	0.01763004	0.00032557	0.00062100	0.53349122	0.01263637
0.00001600	0.01763004	0.00032557	0.00037600	0.33423160	0.00765101
0.00004700	0.04812766	0.00095638	0.00001900	0.02069234	0.00038662
0.00007900	0.07808745	0.00160753	0.00001900	0.02069234	0.00038662
0.00004700	0.04812766	0.00095638	0.00005600	0.05666416	0.00113951
0.00001600	0.01763004	0.00032557	0.00005600	0.05666416	0.00113951
0.00001600	0.01763004	0.00032557	0.00009400	0.09182177	0.00191275
0.00001600	0.01763004	0.00032557	0.00003800	0.03947850	0.00077324
0.00001600	0.01763004	0.00032557	0.00056400	0.48770733	0.01147651
0.00001600	0.01763004	0.00032557	0.00003800	0.03947850	0.00077324
0.00001600	0.01763004	0.00032557	0.00009400	0.09182177	0.00191275
0.00003100	0.03265533	0.00063080	0.00026300	0.23953879	0.00535164
0.00014100	0.13398539	0.00286913	0.00063900	0.54788868	0.01300264
0.00018800	0.17518487	0.00382550	0.00018800	0.17518487	0.00382550
0.00018800	0.17518487	0.00382550	0.00003800	0.03947850	0.00077324
0.00036100	0.32178783	0.00734578	0.00048900	0.42697738	0.00995038
0.00017300	0.16212184	0.00352028	0.00013200	0.12599723	0.00268599
0.00001600	0.01763004	0.00032557	0.00015000	0.14193891	0.00305226
0.00003100	0.03265533	0.00063080	0.00018800	0.17518487	0.00382550
0.00006300	0.06323843	0.00128195	0.00011300	0.10900771	0.00229937
0.00022000	0.20282307	0.00447665	0.00001900	0.02069234	0.00038662
0.00003100	0.03265533	0.00063080	0.00062100	0.53349122	0.01263637
0.00001600	0.01763004	0.00032557	0.00001900	0.02069234	0.00038662
0.00003100	0.03265533	0.00063080	0.00030100	0.27164350	0.00612488
0.00001600	0.01763004	0.00032557	0.00005600	0.05666416	0.00113951
0.00001600	0.01763004	0.00032557	0.00003800	0.03947850	0.00077324
0.00001600	0.01763004	0.00032557	0.00028200	0.25562796	0.00573826
0.00007900	0.07808745	0.00160753	0.00001900	0.02069234	0.00038662
0.00007900	0.07808745	0.00160753	0.00060200	0.51826304	0.01224975
0.00015700	0.14810247	0.00319470	0.00060200	0.51826304	0.01224975
0.00040800	0.36066720	0.00830216	0.00009400	0.09182177	0.00191275
0.00051800	0.45052988	0.01054048	0.00013200	0.12599723	0.00268599
0.00050200	0.43754683	0.01021491	0.00037600	0.33423160	0.00765101
0.00003100	0.03265533	0.00063080	0.00003800	0.03947850	0.00077324
0.00006300	0.06323843	0.00128195	0.00001900	0.02069234	0.00038662
0.00017300	0.16212184	0.00352028	0.00009400	0.09182177	0.00191275
0.00033000	0.29595735	0.00671498	0.00022600	0.20797356	0.00459874
0.00004700	0.04812766	0.00095638	0.00018500	0.97423333	0.02411288
0.00007900	0.07808745	0.00160753	0.00018800	0.17518487	0.00382550
0.00023600	0.21653719	0.00480223	0.00001900	0.02069234	0.00038662
0.00012600	0.12065131	0.00256390	0.00007500	0.07439616	0.00152613
0.00006300	0.06323843	0.00128195	0.00030900	0.68260659	0.01646187
0.00001600	0.01763004	0.00032557	0.00005600	0.05666416	0.00113951

Table C1, Continued

-41-

Table C1, Continued

Flowrate, q at slope bottom	Computed soil loss (lb/ft ²)	Measured soil loss (lb/ft ²)
0.00028200	0.25562796	0.00573826
0.00118500	0.97423333	0.02411288
0.00056400	0.48770733	0.01147651
0.00058300	0.50300212	0.01186313
0.00007500	0.07439616	0.00152613
0.00048900	0.42697738	0.00995038
0.00033800	0.30263851	0.00687777
0.00030100	0.27164350	0.00612488
0.00022600	0.20797356	0.00459874
0.00039500	0.34994540	0.00803763
0.00018800	0.17518487	0.00382550
0.00009400	0.09182177	0.00191275
0.00024400	0.22337028	0.00496502
0.00030100	0.27164350	0.00612488
0.00097800	0.81462137	0.01990076
0.00131600	1.07424318	0.02677853
0.00001900	0.02069234	0.00038662
0.00037900	0.33671625	0.00771205
0.00035700	0.31846367	0.00726439
0.00003800	0.03947850	0.00077324
0.00056400	0.48770733	0.01147651
0.00001900	0.02069234	0.00038662
0.00000000	0.00000000	0.00000000

APPENDIX D

The data in this appendix was collected by John Clouser of Triangle Mining Company, who were contracted with Staffer Chemical Company to do the mining at the Wooley Valley site. Mr. Clouser very generously supplied us with his original copy of this data. Since climatic data is essentially nonexistent in the immediate vicinity of the mine sites, with the nearest available data at Conda and Soda Springs, there appears to be good justification for including the data in this report. We fear, otherwise, it will be lost. The climatic data has been reproduced directly at a reduced size from the hand records that Mr. Clouser generously supplied us, because we believe a loss would result from typing the original data.

MONTH JAN 76

[illegible]

Av Temp 34.4 2.2° F rise

MONTH MARCH 76

Date	Time	Bar. Press.	Time	Bar. Press.	Curr. Temp.	Max. Temp.	Min. Temp.	Precip.	Remarks
1	07:45	23:33	12:00	22:48	23	38	-13	.035	Clear
2	08:30	23:19	15:20	23:19	22	36	-10	0	Clear
3	09:00	23:23	16:00	23:15	17	25	-12	0	Clear
4	08:00	23:20	16:00	23:31	10	38	-14	0	Clear
5	12:30	23:53	16:00	23:61	17				
6									
7						40	-8	0	Clear
8	08:00	23:48	16:00	23:50	28	44	+3	0	Clear
9	08:00	23:47	16:00	23:47	31	52	+8	0	Clear
10	08:00	23:46	16:00	23:37	36	35	12	.04	Snow
11	08:00	23:13	16:00	23:23	18	30	-12	0	Clear
12	08:00	23:60	16:00	23:65	19	44	+1	0	Wg. Sky
13	10:45	23:55	12:15	23:54	32				
14									
15									
16	08:00	23:55	16:00	23:50	54	60	20	0	Clear
17	08:00	23:35	16:00	23:21	48	59	27	.05	Cloudy
18	08:00	23:35	16:00	23:21	48	47	+1	.07	
19	09:00	23:18							
20									
21	09:20	23:65	16:00	23:51	41	56	15	.14	Clear
22	09:00	23:39	16:00	23:42	25	40	21	.17	Cloudy
23	09:00	23:40	16:00	23:30	30	40	15	.09	Stormy
24	09:00	23:40	16:00	24:11	30	41	21	.06	Sat. cfs. 500
25	09:00	23:55	16:00	23:46	33	43	+5	.02	Snow
26	08:00	23:21	12:00	23:20	18	37	+18	.05	Clear
27	10:00	23:21	12:00	23:20	18	46	+7	0.02	Clear
28						32	+7	0	
29	09:00	23:39	16:00	23:53	24	40	+9	0	
30	09:00	23:64	16:00	23:65	30				
31						41	5	.0745	Moisture

Avg. Temp 23 Moisture

Date	Time	Bar. Press.	Time	Bar. Press.	Curr. Temp.	Max. Temp.	Min. Temp.	Precip.	Remarks
1	14:30	23:57	16:00	23:57	29	46	12	0.01	Clear
2									
3									
4									
5	08:00	23:39	16:00	23:30	33	70	12	0.01	Clear
6						48	31	0.01	Clear
7						51	30	0.10	Clear
8	12:45	23:14	17:00	23:54	49	52	25	0.01	Clear
9	08:00	23:31	17:00	23:32	49	53	30	0.10	Clear
10									
11						63	18	0.01	Clear
12	08:00	23:39	16:30	23:33	44	44	19	0.01	Clear
13	10:00	23:29	16:00	23:29	34	44	16	0.01	Clear
14	12:00	23:20	12:00	23:20	42	47	11	0.01	Clear
15	08:00	23:00	17:45	23:05	32	44	22	0.01	Clear
16	07:30	23:32	16:30	23:30	45	52	23	0.07	Clear
17						62	11	0.01	Clear
18	07:45	23:57	18:00	23:40	35	61	18	0.01	Clear
19	08:00	23:56	16:00	23:44	42	50	25	0.01	Clear
20	07:30	23:53	16:00	23:35	54	56	23	0.01	Clear
21	08:00	23:25	16:10	23:21	35	60	24	0.01	Clear
22						56	26	0.01	Clear
23						62	22	0.01	Clear
24						62	12	0.01	Clear
25	08:00	23:21	16:00	23:47	46	52	12	0.01	Clear
26	09:00	23:50	16:00	23:53	76	12	23	0.01	Clear
27									
28									
29									
30									
31						54.6	21.1	16.05	

Avg. Temp 37.88

MONTH MAY 1976

Date	Time	Bar. Press.	Time	Bar. Press.	Curr. Temp.	Max. Temp.	Min. Temp.	Precip.	Remarks
1	09:50	23.42	16:00	23.41	58	69	78	-0-	P. Cloudy
2						69	18	-0-	P. Cloudy
3	09:50	23.42	16:00	23.41	58	68	28	.16	P. Cloudy
4	08:30	23.40	16:00	23.42	46	58	28	.0	Windy Lt. Rain
5	08:30	23.40	16:00	23.40	52	57	39	0.03	Sunny
6	09:30	23.45	15:50	23.50	57	64	30	-0-	SUNNY PLY
7	09:55	23.61	15:55	23.54	60	70	33	-0-	SUNNY CLOUDY
8	09:30	23.58	12:00	23.55	58				Pty Cloudy
9						66	30	0.02	Pty Cloudy
10	09:00	23.62	15:30	23.59	48	57	38	.15	Pty Cloudy
11					55	52	25	-0-	Clear - Wind
12	08:00	23.80	15:45	23.77	50	68	39	0.01	Clear Windy
13	08:30	23.74	16:30	23.65	64			-0-	Clear Windy
14	10:50	23.46	15:50	23.45	65				Sunny
15						76	34	-0-	Sunny
16						73	40	0	Sunny Wind
17	08:30	23.57	16:40	23.54	72	75	33	-0-	Windy
18	08:30	23.47	16:00	23.43	71	70	30	-0-	P. Cloudy
19	08:30	23.43	16:20	23.49	67	70	30	TR	Windy - Rain
20					45	45	43	0.32	Pty Cloudy
21			16:20	23.50	62	41	35	0.32	Windy - Rain
22	11:15	23.48	13:15	23.47	44	58	38	.05	Pty Cloudy
23						59	36	.07	Sunny - Wind
24	08:20	23.48	16:00	23.46	52	60	27	-0-	Sunny - Wind
25	09:00	23.42	16:20	23.44	52	68	30	-0-	Sunny - Wind
26	15:32	23.63	16:50	23.63	58				
27	08:00	23.61	16:00	23.55	68				
28									
29									
30									
31									

Ave - 23.53 Ave - 23.51 Ave 58° Ave 64.5 Ave 33.7° Ave 48.1° 1.13"

MONTH June 1976

Date	Time	Bar. Press.	Time	Bar. Press.	Curr. Temp.	Max. Temp.	Min. Temp.	Precip.	Remarks
1	09:00	23.53	16:20	23.50	66	82	31	-0-	P. Cloudy
2	08:00	23.54	16:20	23.50	69	75	42	0	P. Cloudy
3	08:00	23.43	16:00	23.42	69	76	40	0	P. Cloudy
4									
5									
6						80	34	-0-	Hi. Cld. Sunny
7			16:50	23.46	75	80	51	-0-	Hi. Cld.
8	09:00	23.50	16:15	23.46	70	72	41	-0-	Sunny
9	08:00	23.52	16:30	23.50	68	70	44	TR	Cloudy - Thir.
10	09:50	23.37	16:40	23.54	50	50	37	0.20	Stormy Rain
11			16:30	23.38	38	42	39	0.02	CLOUDY - Rain
12	10:00	23.45	12:00	23.45	40	52	27	0.01	Snowy
13	09:00	23.41				47	27	.50	Pty Cloudy
14	09:00	23.61	16:00	23.60	42	60	26	0	Clear
15	08:00	23.71	16:00	23.63	57	55	40	0.12	Pty Cld - Shurs
16	08:00	23.40	16:45	23.41	39	59	33	0.63	Rain Hi!
17	08:00	23.51	16:50	23.69	56				
18						92	32	-0-	Sunny - Thir. Shurs
19	10:00	23.65	16:30	23.66		92	32	-0-	Sunny " "
20			19:24	23.60	57	90	37	0.10	Thir. Shurs
21						54	37	0.01	Cldy - Lt. Snow
22	08:00	23.46	16:15	23.49	49	53	36	TR	CLOUDY
23	09:30	23.55	15:50	23.59	46	58	27	0.04	Pty Cldy
24	08:00	23.64	17:15	23.54	56	60	46	0.00	Windy - Cold
25	15:00	23.43	16:30	23.46	54	57	24	-0-	Hi. Clouds
26	16:00	23.64	12:30	23.69	49	78	27	-0	Sunny
27						79	27	-0-	Sunny
28	09:50	23.76	16:00	23.77	75	93	43	-0-	Hot
29	08:00	23.67	16:00	23.64	83	88	50	-0-	Sunny
30	08:00	23.54	16:00	23.54	76				
31						104.42			

Ave = 60.45 Ave 68.5 Ave 35.92 Ave 1.63" 52.2°

MONTH July 1976

Time	Bar. Press.	Time	Bar. Press.	Curr. Temp.	Max. Temp.	Min. Temp.	Precip.	Remarks
					94	36	-0-	Hazy-Hot
1 14:49	23.55	16:00	23.50	69				
3		18:00	23.64	78	88	29	-0-	Ptly. Cldy - Clr
5					96	42	-0-	
6 08:30	23.67	16:00	23.65	89	95	42	-0-	Clear - Hot
7 08:00	23.60	16:30	23.57	80	107	50	-0-	Hi clouds - Hot
8 08:00	23.57	16:00	23.58	82	95	50	-0-	Clear - Hot
9 08:00	23.60	—	—	—	100	46	-0-	Clear Hot
10 13:00	23.63	14:48	23.64	74	80	46	-0-	Clear Hot
11					87	51	-0-	Clear
12 08:00	23.47	16:30	23.50	68	75	41	-0-	Clear
13 08:00	23.60	16:30	23.60	69	74	41	-0-	Clear
14 08:00	23.61	16:00	23.63	73	80	38	-0-	
15 08:00	23.71	16:30	23.69	78	87	43	-0-	
16 08:00	23.74	16:17	23.73	83				
17					82	45	0.43	blowburst
18					66	45	0.03	Clear
19 09:00	23.66	16:30	23.65	66	74	42	0	Clear
20 08:00	23.73	16:30	23.70	70	75	44	0	Clear
21 09:00	23.62	16:30	23.68	50	80	45	0.04	Light Shower
22 08:00	23.67	16:30	23.70	40.78	88	45	-0-	Hot
23 08:00	23.77	16:00	23.76	87	86	50	-0-	Light Cls
24 14:00	23.75	16:00	23.72	72		45		Clear
25		11:30	23.74	64	77	50	TR	Ptly. Cloudy
26 12:00	23.65	16:00	23.64	59	78	44	-0-	Windy - Hot
27 12:00	23.64	17:00	23.60	75	76	41	-0-	Hi Clouds
28 12:00	23.61	17:00	23.58	78.75	80	50	-0-	Hi Clouds
29 12:00	23.58	17:00	23.59	74	77	47	-0-	Hi Clouds
30 08:30	23.60				76	50	0.20	Light Shower
31 11:00	23.62	15:30	23.69	79	83.5	44.2	0.04	

83.5 Ave 43.8 0.74

MONTH August 1976

Time	Bar. Press.	Time	Bar. Press.	Curr. Temp.	Max. Temp.	Min. Temp.	Precip.	Remarks
8:05	23.72				74	43	0	
8:05	23.72	16:30	23.66	75	72	42	0.15	Ptly. Cloudy
10:00	23.66	16:30	23.67	67	74	39	0	Ptly. Cloudy
2:00	23.63	16:30	23.63	66	73	35	0	Ptly. Cloudy
10:00	23.67	16:30	23.65	67	82	40	0	Clear
		16:30	23.61	75	77	40	-0-	Clear
10:30	23.55	15:30	23.55	71	73	33	-0-	Clear
09:45	23.55	11:20	23.55	66	73	35	-0-	Clear
08:15	23.58	16:30	23.60	65	69	41	-0-	Clear
07:15	23.64	18:00	23.65	66	74	39	-0-	Ptly. Cloudy
08:00	23.73	16:00	23.73	60	78	38	-0-	Hi Clouds
08:00	23.74	17:00	23.68	75	75	37	-0-	Scat. Clouds
08:00	23.62	16:40	23.50	69	76	40	-0-	Windy Windy
10:00	23.44	11:00	23.42	68	78	40	0.29	Rain
5					65	39	0.00	blowburst
6 08:00	23.53	16:30	23.55	63	71	40	—	Ptly. Cldy
7 07:40	23.65	16:30	23.55	71	71	48	.21	Cloudy
8 08:00	23.60	16:30	23.60	61	70	44	-0-	Clear
9 08:00	23.65	16:20	23.64	68	75	40	0	Clear
10 08:00	23.64	16:00	23.65	75	79	40	-0-	Clear
11		12:37	23.68	77	82	45	0.34	Rain PM
2 07:30	23.64				62	48	0.06	
3 07:30	23.64	16:30	23.60	59	72	33	0	Clear
4 08:00	23.76	16:30	23.75	70	75	41	0	Clear
5		16:00	23.67	73	75	41	0	Ptly. Cloudy
6 07:00	23.62	16:00	23.62	59	63	26	0	Clear
7 08:00	23.74	16:00	23.77	60	76	26	0	Clear
8 09:15	23.82	16:30	23.82	75				
9		16:00						
10 08:00	23.76	16:00	23.75	73	78	39	0	Clear
11 05:00	23.80	16:00	23.77	74	75	40	0	Clear
Ave					68.7°	73.7°	39.2°	1.05"

MONTH *Sept 1976*

Date	Time	Bar. Press.	Time	Bar. Press.	Curr. Temp.	Max. Temp.	Min. Temp.	Precip.	Remarks
1	08:00	23.77	16:00	23.73	77	78	40	0	Clear Warm
2	08:00	23.65	16:00	23.65	78	80	44	0	Clear Warm
3	08:00	23.61	16:00	23.66	78	79	41	-0	Clear "
4	7:55	23.58	16:00	23.58	77	79	37	-0	Clear "
5	12:30	23.62	14:50	23.59	85	87	40	-0	Clear Windy
6	08:00	23.65				85	28	-0	
7	08:00	23.65	16:30	23.66	56	63	28	.33	Clear Cool
8	08:00	23.80	16:00	23.82	56	58	23	0	Clear Cool
9	08:00	23.87	16:30	23.82	68	70	24	0	Clear Cool
10	08:00	23.73	16:00	23.65	74	74	35	0	Clear Warm
11	08:00	23.55	16:00	23.48	65	75	56	T	Cloudy Windy
12	11:50	23.58				65	51	.22	Cloudy Rain
13	08:00	23.70	16:00	23.67	62	66	31	0	Clear
14	08:00	23.67	16:30	23.62	64	67	32	0	Clear
15	08:00	23.60	16:30	23.58	65	71	38	0	Part Cloudy
16	08:00	23.58	16:30	23.58	71	74	47	0.01	Clear
17	08:00	23.60	16:30	23.56	86	72	44	.01	Part Cloudy
18	07:25	23.60				66	35	0.03	Part Cloudy
19									
20	12:00	23.13	16:40	23.70	66	70	30	-0	Sunny
21	08:00	23.67	16:30	23.62	65	70	31	0	Clear
22	08:00	23.60	16:30	23.59	43	69	45	.03	Cloudy
23	08:00	23.61	16:30	23.60	59	68	34	0	Cloudy
24	09:00	23.64	16:30	23.61	60	64	34	0	Cloudy
25	08:00	23.53	16:30	23.51	44	65	35	.25	Rain
26									
27	09:00	23.60	16:20	23.57	60	64	32	0.02	Part Cloudy
28	08:00	23.58							
29	08:00	23.63	16:30	23.63	67	69	27	0	Clear
30	08:00	23.60	16:30	23.59		70	30	-0	
31									

Mo 70 No 35
Mo 52.5 0.68

MONTH *October 1976*

Date	Time	Bar. Press.	Time	Bar. Press.	Curr. Temp.	Max. Temp.	Min. Temp.	Precip.	Remarks
1	8:00	23.59	17:00	23.50	66	75	31	-0	Clear
2									
3									
4	09:00	23.55	17:00	23.57	40	46	27	0.30	Rain
5	09:00	23.62	15:40	23.60	43	46	23	.02	Part Cloudy
6	11:30	23.67	17:00	23.70	44	47	28	-0	Clear
7	08:00	23.80	16:30	23.77	50	51	20	-	Clear
8	08:00	23.78	16:30	23.75	61	62	22	-	Clear
9	08:00	23.75	17:20	23.83	62	65	23	-0	Clear
10									
11	08:00	23.55	16:00	23.60	53	66	30	0	Part Cloudy
12	08:00	23.70	16:00	23.80	54	57	25	0	Clear
13	08:00	23.72	16:12	23.73	60	62	24	0	Sunny
14	08:00	23.54	16:15	23.47	59	60	30	0	Sunny
15	15:00	23.49	17:20	23.50	55	60	26	0	Sunny
16	11:40	23.60	14:20	23.59	55	55	23	0	Sunny
17									
18	08:00	23.54	16:00	23.64	39	56	10	0	Sunny
19	08:00	23.70	17:00	23.68	42	44	10	0	Sunny
20	07:00	23.70	16:10	23.66	53	53	15	0	Sunny
21	08:00	23.64	16:30	23.54	54	56	19	0	Sunny
22	08:00	23.46	16:30	23.41	48	55	19	0	Sunny
23									
24									
25									
26									
27	08:00	23.64	16:30	23.69	30	48	16	0.30	Sunny
28	08:00	23.64	17:00	23.70	33	39	02	-0	Sunny
29	08:00	23.69	17:00	23.60	41	45	15	-0	Sunny
30	08:00	23.60	17:00	23.57	44	48	18	-0	Hi Cl.
31									

Mo 70 No 35
Mo 52.5 0.68
Avg Temp 37.4 61.1 Mo 1.5 F

MONTH Nov '76

Day	Time	Bar. Press.	Time	Bar. Press.	Curr. Temp.	Max. Temp.	Min. Temp.	Precip.	Remarks
1	07:00	23.72	16:30	23.74	46	51	26	0	Part Cloudy
2	07:00	23.71	16:30	23.76	50	53	20	0	Clear
3	07:00	23.71	16:30	23.76	50	56	22	0	Clear
4	07:00	23.71	16:30	23.65	50				
5	07:00	23.71	16:30	23.65	50				
6									
7						58	25	0	Clear
8	07:00	23.73	16:00	23.71	46	53	22	0	Clear
9	07:00	23.74	16:00	23.64	45	49	25	0	Clear
10	07:00	23.74	16:30	23.62	47	50	17	0	Clear
11	07:00	23.75	16:00	23.55	50	51	17	0	Clear
12	07:00	23.75	16:00	23.54	45				
13									
14						46	9	0	Cloudy-Snowy
15	07:00	23.74	16:45	23.60	26	42	30	0.02	Cloudy Cold
16			16:00	23.74	37	49	34	0	Clear
17	07:00	23.74	16:30	23.75	44	48	28	0	Partly Cloudy
18			16:00	23.58	44				
19	07:00	23.60							
20									
21						46	13	0	Clear
22	07:00	23.64	16:00	23.73	40				
23									
24									
25									
26						40	-12	.05	
27									
28						40	8	0	Partly Cloudy
29	07:00	23.72	16:00	23.75	18	38	13	0	Clear
30	07:00	23.72	16:00	23.77	17				
31									
Ave.					39.5°	48.5°	19.0°	.07"	
						33.7			

MONTH Dec 76

Date	Time	Bar. Press.	Time	Bar. Press.	Curr. Temp.	Max. Temp.	Min. Temp.	Precip.	Remarks
1	07:00	23.86	16:00	23.74			6	0	
2			16:00	23.72	35	42	10	0	Clear
3	07:00	23.71	16:00	23.62	31	40	14	0	
4									
5						32	4	0.23	
6	07:00	23.62	16:00	23.63	20	25	4	0	Cloudy
7	07:00	23.60	16:00	23.57	20	23	19	.03	Partly Cloudy
8	07:00	23.55	16:30	23.42	18	42	23	-R-	Snow
9									
10	07:00	23.70	16:00	23.73	27	26	0	.03	Clear
11									
12			12:00	23.69	31	38	4	0	Sunny
13	07:00	23.64	17:00	23.52	28	41	12	0	Highly
14	07:00	23.64	16:00	23.62	30	42	10	0	Clear
15	07:00	23.74	16:00	23.75	30	41	9	0	Clear
16	07:00	23.75	16:00	23.66	34	44	12	0	Clear
17	07:00	23.50	16:00	23.45	42	48	12	0	Clear
18									
19									
20	07:00	23.69				44	0	0	Clear
21			15:40	23.52	25	44	0	0	Heavy High
22	07:00	23.54	16:30	23.58	20	35	0	0	Cloudy
23			16:00	23.38	24	35	7	0	
24									
25									
26						42	4	0.015	Snow Xmas
27	10:00	23.44	16:00	23.45	22	32	3	0	Heavy Snow
28	12:00	23.62	17:00	23.62	24	36	3	-0--	Heavy Snow
29	09:00	23.38	15:40	23.33	30	38	3		Cold
30	08:30	23.24				34	1		Heavy Cold
31	13:00	23.23	14:30	23.20	19	23	1		Heavy Cold
						35.7AV	6.7AV	.305	
						21.2			

MONTH

AV $31^\circ + 5^\circ$ 0.972
18°

MONTH February 1911

39.8 Hi	9.9 Lo	0.43
---------	--------	------

MONTH March 1977

Date	Time	Bar. Press.	Time	Bar. Press.	Curr. Temp.	Max. Temp.	Min. Temp.	Precip.	Remarks
1	08:00	23.19	16:20	23.12	16	35	16	0.03	Snow
2	0800	23.14	1620	23.21	20	23	13	0.03	Snow Flurries
3	08:00	23.27	1615	23.34	21	34	13	0.04	Snow Flurries
4	0800	23.49	16:15		20	26	05	0.01	
5							.06	-0-	
6	0830	23.61	16:15	23.57	40	48	21	-0-	
7	0930	23.52	1500	23.51	28	42	11	-0-	Snow
8	0900	23.31	1500	23.18	29	38	22	-0-	Snow
9	08:00	23:30	1615	23.47	22	29	-5	0.075	Windy
10	0800	23.69	1630	23.66	26	30	0	-0-	Clear Cold
11						25	0	0	Hi. Windy
12	08:00	23.50	10:30	23.40	35	48		0.07	Cloudy
13	0800					25	-1	-0-	Flurries
14	0800	23.27	16:30	23.17	14	38	2	.01	Cloudy
15	0800	23.50	1630	23.50	30	40	19	-0-	Snow
16	0800	23.40	1630	23.25	31	23	15	T ₀ .04	
17	0800	23.13	1600	23.24	19		1	0.10	
18	13:00	23.13							
19									
20									P. Cloudy
21	0800	23.57	1600	23.61	32	38	03	.15	Clear
22	08:00	23.58	1630	23.56	52	55	18	0	P. Cloudy
23	08:00	23.35	1630	23.21	46	52	20	0	Snow
24	0800	23.24	1630	23.25	30	47	22	.16	Flurries
25	08:00	23.13	1615	23.21	24	30	24	.03	Hi. Windy
26	11:30	23:35	14:00	23:36	34	36	10	.03	
27	0800	23.17							Cloudy
28	08:00	23:17	16:10	23:15	18	30	6	.04	Cloudy
29	0900	23.18	16:30	23.23	13	31	7	.10	Cloudy
30	0900	23.47	1630	23.50	34	30	0	.01	Flurries
31	0800	23.40	1630	23.30	27	40	6	0	
Avg. - 27.5°						34.9	9.6°	1.00"	

MONTH April 1977

Date	Time	Bar. Press.	Time	Bar. Press.	Curr. Temp.	Max. Temp.	Min. Temp.	Precip.	Remarks
1	0800	23.11	16:20	23.10	30	32	21	.08	Snow
2	0800	23.21				35	12	.04	Flurries
3									
4	0800	23.60	1630	23.66	39	39	15	0	Sunny
5	0800	23.68	1630	23.71	46	47	26	0	"
6	10:00	23.77	1630	23.74	56	58	22	0	"
7			17:30	23.69	50	66	25	0	
8	0800	23.64	1600	23.54	60	62	27	0	Hi. Windy
9			19:00	23.87	38	60	42	0	Clear
10	12:00	23.49	18:05	23.49	42	47	24	0	Clear Windy
11	0800	23.52	17:00	23.46	47	51	19	0	Clear
12			16:30	23.60	48	51	24	0	Hi. Windy
13	0800	23.50	17:00	23.40	46	52	22	0	
14	0800	23.32	16:00			48	27	0	
15	0800	23.57	16:00	23:54	52	55	23	.05	Clear Warm
16									Hi. Windy
17	11:00	23.50	11:00		38	38	27	-0-	Clear Sunny
18	0800	23.49	1630	23.43	36	41	17	.07	Sunny - Cold
19	08:00	23.43	1630	23.44	40	42	16	0	Hi. Windy
20	0900	23.47	1630	23.48	47	48	18	0	Cloudy
21	0800	23.58	16:00	23.58	50	56	28	0	Sunny
22	10:00	23.70	16:30	23.69	44	66	25	0	
23						74	34	0	P. Cloudy
24	0					72	34	0	P. Cloudy
25	0800	23.65	1600	23:60	65	67	34	0	P. Cloudy
26	0800	23.56	1630	23:50	59	66	33	0	P. Cloudy
27	0800	23.51	1630	24:49	60	63	35	0	P. Cloudy
28			16:00	23:54	55	64	35	0	P. Cloudy
29	09:30	23:60	1600	23:56	58			.15	
30	0900	23.55				70	30	.02	
31						(54.4)	(25.7)	0.41"	
Avg. - 23.55						39.8			

MONTH May 1977

Date	Time	Bar. Press.	Time	Bar. Press.	Curr. Temp.	Max. Temp.	Min. Temp.	Precip.	Remarks
1								<u>.72</u>	Rain
2	08:30	23.55	16:00	23.52	50	58	30	.05	Wind + Windy
3	08:10	23.37	16:00	23.28	50	59	33	.01	Snow
4	09:00	23.32	16:30	23.33	17	54	27	0.18	Snow-Squalls
5	09:00	23.28	16:30	23.20	39	40	20	.05	Light Rain-Snow
6	08:00	23.20	12:30	23.28	38	45	31	.44	
7									
8						59	30	.01	
9	08:00	23.42	14:00	23.30	65	70	30	-0-	Snow + Rain
10	08:00	23.33	16:00	23.35	40	68	33	0.10	Clear + Wind
11	08:00	23.40	16:00	23.37	52	56	28	.02	P. Cloudy
12	08:00	23.47	16:30	23.47	60	57	27	.01	P. Cloudy
13	08:00	23.45	16:00	23.40	60	68	29	0	
14	08:00	23.24							
15						38	32	.15	Rain
16	08:00	23.24	16:00	23.22	32	46	32	0.15	Rain + Hail
17	08:00	23.30	16:00	23.40	44	53	29	.63	Snow
18	08:00	23.37	16:00	23.41	31	33	28	.08	Flurries
19	08:00	23.50	16:00	23.42	38	44	30	.30	Light Snow
20	08:00	23.57			36	48	28	.31	Snow Showers
21									
22						57	28	.04	Snow Showers
23	08:00	23.29	15:45	23.28	58	63	28	-0-	Light Windy
24	08:00	23.33	17:00	23.30	42	49	34	TR	Windy
25	07:30	23.37	14:00	23.33	41	47	31	.26	Snow + Rain
26	08:00	23.42	14:30	23.37	47	51	29	.18	Rain
27	08:00	23.40				64	32	.16	Rain Snow
28									
29									
30									
31	09:24	23.77	16:00	23.77	72	72	44	.02	Sunny

AV - 41.9

MONTH June 1977

Date	Time	Bar. Press.	Time	Bar. Press.	Curr. Temp.	Max. Temp.	Min. Temp.	Precip.	Remarks
1	08:00	23.66	16:30	23.60	70	77	38	-0-	Clear
2	08:00	23.58	16:20	23.55	67	70	42	-0-	Clear
3	08:00	23.55	16:30	23.57	72	74	43	-0-	Clear
4						82			
5						80	43	-0-	Clear
6	08:00	23.74	16:30	23.71	71	80	50	-0-	Clear
7	08:00	23.67	16:00	23.60	79	76	45	-0-	P. Cl.
8	08:00	23.52	16:30	23.50	74	75	49	.21	Thunder Storm
9	08:00	23.42	16:00	23.42	64	76	45	.10	Shower
10	08:00	23.50	16:00	23.57	51		45	.05	Snow
11	11:00	23.56			63				
12									
13	08:00	23.56	16:00	23.53	69	71	40	0	P. Cloudy
14	08:00	23.54	16:00	23.55	70	73	42	0	P. Cloudy
15	10:00	23.65	16:30	23.63	65	70	35	0	P. Cloudy
16	08:00	23.60	16:00	23.60	70	73	38	0	P. Cloudy
17	08:00	23.61	16:30	23.61	69	74	41	0	P. Cloudy
18	08:00	23.48						.13	
19									
20	08:00	23.48	16:00	23.50	50	60	37	.16	Light Snow
21	08:00	23.56	16:00	23.57	62	66	36	-0-	Light Snow
22	09:00	23.58	16:00	23.60	70	72	40	-0-	Light Snow
23	08:00	23.66	16:00	23.66	70	78	41	-0-	PIT Cloudy
24	08:00	23.66					44		
25									
26			17:15	23.60	70	54	44	0	Sunny
27	08:00	23.67	16:00	23.67	74	76	48	0	Sunny
28	08:00	23.75	16:30	23.67	72	76	40	0	Windy
29	12:30	23.58	16:30	23.57	69	76	42	0	Sunny
30			16:10	23.60	70	72	35	-0-	Sunny
31						73.1	41.6	0.52	Thunder

Avg Temp 57.3° 0.52"

MONTH <i>July 1977</i>									
Day	Time	Bar. Press.	Time	Bar. Press.	Curr. Temp.	Max. Temp.	Min. Temp.	Precip.	Remarks
1									
2									
3									
4						75			
5	0800	23.56	1600	23.60	71	74	38	.70	11 Cloudy
6	0800	23.67	1430	23.68	67	69	39	.01	Wind 1. Cloud
7	08:00	23:71	16:45	23.69	70	70	35	-0-	Windy-Sunny
8	08:30	23.64	1600	23.60	75	77	40	-0	Windy-Cloudy
9	08:00	23.60				80	55	-0-	
10									
11	08:00	23:63	16:00	23.63	70	72	36	-0-	Sunny-Breeze
12	07:45	23:60	16:00	23:57	78	80	45	-0-	Sunny-Warm
13	08:00	23:57	16:00	23:62	70	70	56	-0-	PHY - Windy
14			16:30	23.68	72	74	34	-0	Sunny-Windy
15	08:00	23.70	18:00	23.69	72	83	41	-0-	Sunny-Windy
16									
17						85	50	-0-	Hot-Windy
18	0930	23.59	16:00	23.57	81	83	67	-0-	Hot!!
19	1630	23.57	17:00	23.57	76	84	60	-0-	Hot-Windy
20	0630	23.67	16:30	23.67	80	85	52	-0-	Hot Wind
21	07:45	23.85	16:30	23.71	75	80	54	0.20	Hot Wind
22	07:45	23.74	17:50	23.70	66	81	46	0.19	Hot Wind
23	14:00	23.70	16:00	23.68	66	82	55	0.02	Hot Wind
24						73	43	0.39	Hot Wind
25	07:30	23.74	16:00	23.77	73	73	43	-0-	Clear
26	08:00	23.76	16:45	23.75	70	80	45	-0-	Clear
27	07:40	23.75	17:00	23.72	71	76	43	-01	Sunny
28	07:45	23.73	16:15	23.71	76	82	43	-0-	Sunny
29	08:00	23.68	16:30	23.70	72	75	49	-0	Clear
30	10:45	23.75	15:15	23.70	71	73	38	-0	Hot-Sunny
31						76	37	-0	Hot
						77.5	45.7		
						Av. 61.6		1.43"	

MONTH <i>July</i>									
date	Time	Bar. Press.	Time	Bar. Press.	Curr. Temp.	Max. Temp.	Min. Temp.	Precip.	Remarks
1	08:45	23.79	16:30	23.78	79	80	37	-0-	Hot Sunny
2	06:45	23.75	15:45	23.72	77	83	45	-0-	Hot Sunny
3	06:45	23.66	15:45	23.61		82	49	-0-	Hot
4	08:30	23.63	16:30	23.58	75	80	50	-0-	Hot
5	08:30	23.62	16:00	23.60	65	74	50	-0.01-	Cloudy
6									
7						79	38	0.34	
8	07:45	23.60	16:00	23.63	67	70	38		Cloudy
9	07:20	23.65	16:30	23.65	74	76	39	-0-	
10	07:20	23.66	16:00	23.65	74	78	40	-0-	
11	07:50	23.70	16:30	23.68	74	78	42	-0-	Clear Hot
12			16:20	23.62	77	80	40	-0-	Clear Hot
13	10:30	23.60	16:30	23.51	78	79	46	-0-	Windy Sunny
14						84	46	0.01	Sunny Hot
15	08:00	23.64	16:00	23.61	76	81	46	-0-	Sunny Hot
16	15:45	23.69	16:45	23.69	78	81	44	-0-	Sunny Hot
17	09:00	23.75	16:30	23.73	69	79	48	-0-	Cloudy
18	08:00	23.70	16:50	23.71	60	60	52	0.11	Hot Rain
19	08:00	23.73	16:30	23.72	75	76	45	0	Hot Sunny
20	09:00	23.73					45		Sunny
21									Thunder Storm
22	09:00	23.65	16:00	23.60	53	80	45	0.05	Thunder Storm
23	08:00	23.60	14:30	23.58	53	76	43	.12	Sunny
24			16:30	23.50	48	58	46	-0-	
25	0800	23.54	16:30	23.50	48	58	41	.29	Cloudy Storm
26	0800	23.40	16:00	23.40	44	50	42	.72	Rain
27	0900	23.52	14:00	23.55	47	50	36	.01	
28						56	39	0.10	Cloudy
29	08:00	23.64	16:30	23.60	62	64	39	-0-	Windy Hot
30	0800	23.52	16:00	23.47	58	63	31	-0-	Cloudy
31	0800	23.59	16:30	23.55	63	66	29	0	Hot
						77.5	45.7	2.17"	
						57.4			

MONTH Sept 77

date	Time	Bar. Press.	Time	Bar. Press.	Curr. Temp.	Max. Temp.	Min. Temp.	Precip.	Remarks
1	09:00	23:60	16:00	23:65	64	66	40	0.02	Sunny
2	08:30	23:67	16:00	23:68	73	73	40	-	
3									
4						80	40	-0-	Hot Sunny
5						80	40	-0-	Hot Sunny
6	09:00	23:73	16:30	23:70	76	80	45	-0-	Scat Cls
7	10:30	23:74	16:30	23:69	76	60	57	0-	Cool Windy
8	08:00	23:65	15:30	23:72	60	67	24	-0-	Clear
9	08:30	23:70	16:30	23:67	67	73	3	-0-	Clear
10	09:00	23:64	15:00	23:63	73			TR	
11						64	39	-0-	Pt Cloudy
12	08:00	23:55	16:30	23:59	62	70	30	-0-	Pt Cloudy
13	08:00	23:67	16:30	23:61	68	62	30	0.13	Pt Cloudy
14	08:00	23:57	16:00	23:40	57	63	47	-0-	Cloudy
15	08:00	23:40	16:00	23:37	56	58	40	.01	Cloudy
16			17:00	23:34	57	43	32	0.13	SUNNY
17	09:15	23:44	16:00	23:56	41	59	25	-0-	Windy
18	09:00	23:65	12:00			66	34	-0-	Windy
19	08:00	23:50	16:00	23:43	57	51	35	-0-	Windy
20	07:00	23:47	17:00	23:48	40	52	21	.95	Sunny
21	08:00	23:55	16:30	23:59	51	36	36	0.21	Pt Cloudy
22	08:00	23:45	16:00	23:39	34	47	28	0.13	Cloudy
23	08:00	23:52				44	32	0.01	Pt Cloudy
24	11:00	23:34	13:00	23:39	36	61			Pt Cloudy
25	05					64	31	0	Pt Cloudy
26	08:00	23:45	16:30	23:48	59	67	31	0	Pt Cloudy
27	09:00	23:57	16:30	23:53	65	66	41	0	Pt Cloudy
28	08:00	23:55	16:00	23:53	62	62	42	0	Pt Cloudy
29	09:30	23:46	16:00	23:40	58	35	26	0.09	Sunny
30	09:00	23:43	16:30	23:53	27				
31									

41.1 34.2 1.16"
Avg 48.0

MONTH Oct 77

date	Time	Bar. Press.	Time	Bar. Press.	Curr. Temp.	Max. Temp.	Min. Temp.	Precip.	Remarks
1	1000	23:64				58	30	.12	Snow
2						58	22	-0-	Sunny
3		23:55	17:00	23:58	54	57	22	-0-	SUNNY
4	09:00	23:58	16:00	23:60	54	62	28	-0-	Ptly Cloudy
5	08:00	23:56	17:00	23:54	60	56	44	.03	Cloudy
6	09:00	23:52				43	26		Sunny
7	09:00	23:57	15:30	23:56	41				
8	0800					49			
9						47	22	.03	
10	0800	23:54	1600	23:56	45	59	14	0	
11	0800	23:80	1600	23:76	51				
12									
13									
14									
15									
16									Clear
17	1000	23:52	1630	23:70	60	66	30	0	Clear
18	10:00	23:58	16:30	23:55	62	64	25	TR	Cloudy
19	06:45	23:52	17:15	23:50	47	54	38	-0-	Cloudy
20	0800	23:54	1700	23:60	46	54	27	0	Hi Cloud
21	11:00	23:74	16:00	23:49	54	55	24	-0-	Sunny
22									
23						54	24	-0-	Sunny
24						54	24	-0-	Cloudy
25	11:00	26:67	12:00	23:66		62	31	-0-	Cloudy
26	0800	23:70	1630	23:66	60	61	34	-0-	Sunny
27	09:00	23:57	16:30	23:54	59	62	30	-0-	Sunny
28	12:00	23:49	16:00	23:46	57	56	38	-0-	Sunny
29	10:00	23:55	17:00	23:54	52				
30									
31	08:30	23:47	16:30	23:47	25	30	17	.19+02	Sunny

41.1 34.2 1.16"
Avg 48.0